Storm Gloria (2020): coexisting types of compound flooding in the West Mediterranean Region

Montserrat Llasat-Botija[1,2], Raül Marcos-Matamoros[1], Maria Aguilera-Vidal[3], José Antonio Jimenez[3], María Carmen Llasat[1,2]

[1]GAMA, Department of Applied Physics, Universitat de Barcelona, Barcelona, 08028, Spain
[2]IdRA, Water Research Institute, Universitat de Barcelona, Barcelona, 08028, Spain
[3]Laboratori d'Enginyeria Marítima, Universitat Politècnica de Catalunya, BarcelonaTech, Barcelona, 08034, Spain

Correspondence to: Montserrat Llasat-Botija (mllasat@meteo.ub.edu)

Abstract. Compound flooding arises from the interaction of multiple hydrometeorological drivers, producing impacts that exceed those expected from individual hazards. Although different types of compound events have been widely described, they may also occur simultaneously during exceptional meteorological episodes affecting large regions. Storm Gloria, which struck the Spanish Mediterranean coast between 19 and 25 January 2020, provides a paradigmatic example, as multivariate, spatially compound, and temporarily compound events developed concurrently across the region. The event affected 770 municipalities, caused 14 fatalities and three missing persons and generated about EUR_{2022} 204 million in Spain's Insurance Compensation (CCS) payouts. The analysis combines daily precipitation ($P_{(24h)}$; 662 AEMET rain gauges), maximum wind gusts (140 AEMET stations), and significant wave height (H_s; 50 SIMAR/CoExMed points) with municipality-level CCS compensation data associated with floods, windstorms and coastal flooding, respectively. The event window is objectively defined (≥ 40 mm day^{-1} at ≥ 2 stations), and hazard severity is mapped using operational thresholds (P_{24h} = 40/100/200 mm; H_s = 2/5/7 m; wind gusts ≈ 70/90/100 km h^{-1}). The probability of multivariate and spatially compound events was quantified using a two-sided conditional framework and copula models, while the temporally compounding case was assessed empirically from a sequence of heavy-rainfall episodes. The results show that accounting for the dependence between hazards substantially reduces the estimated return periods of multivariate and spatially compound compared with an assumption of independence. Overall, if the spatial distribution of damages is considered throughout the region, the largest compensation values tend to occur where hazard levels are the highest, although exposure (including insurance coverage) and vulnerability modulate the final impacts. In this event, flooding accounts for the largest share of compensation payments. Beyond documenting an exceptional storm, this study demonstrates how different types of compound events can coexist within a single atmospheric episode and presents an integrated framework linking hazard characterisation, joint probability analysis, and

observed impacts that can support compound-aware coastal flood risk assessment in Mediterranean and other coastal regions.

1 Introduction

Between 19 and 25 January 2020, Storm Gloria severely impacted eastern Spain. This storm developed south of the Iberian Peninsula (IP) and was the seventh named storm of the 2019–2020 season (AEMET, 2025). Owing to its spatial extent and its intensity, the unusual time of year it occurred, and the diversity of associated hazards recorded, Gloria is widely regarded as one of the most remarkable Mediterranean storms in recent decades (Khodayar et al., 2025). It affected large areas of Catalonia, the Valencian Community, the Region of Murcia, parts of Andalusia, Aragon, and the Balearic Islands.

The episode was characterised by persistent heavy rainfall, high river discharges, energetic wave conditions, elevated coastal water levels, strong winds, thunderstorms, hail and snowfalls. The interaction of these drivers generated pluvial and fluvial flooding, flash floods, coastal flooding, coastal erosion and numerous landslides. According to the Insurance Compensation Consortium (*Consorcio de Compensación de Seguros*, CCS), total economic losses across Spain exceeded EUR_{2022} 204 million (EUR_{2022} is the monetary value expressed in constant 2022 euros). In total, more than 900 municipalities were affected, the event caused 14 confirmed fatalities and three missing persons (AEMET, 2025; Luján López, 2022; Gobierno de España, 2020).

The Gloria event is widely considered as a paradigmatic compound event. The analysis of these types of events from a "compound" perspective is not new. The report "Managing the Risks of Extreme Events and Disasters to Advance Climate Change Adaptation" (IPCC, 2012) was one of the first to consolidate the concept of "compound events". Shortly thereafter, Leonard et al. (2014) proposed a framework for the systematic analysis of such events using influence diagrams for defining, mapping, analysing, modelling, and communicating the risk of the compound event. Since then, interest in this topic has grown significantly within the scientific community due to the substantial socio-economic impacts of compound events and their potential increase under climate change (Moftakhari et al., 2017; Bevacqua et al., 2019). Compound events are broadly defined as the combination of weather or climate events and/or hazards that jointly contribute to societal or environmental risk (Seneviratne et al., 2012; Zscheischler et al., 2020; Green et al., 2025). Although these event combinations all have the potential to amplify impacts, they differ in their physical mechanisms and in their implications for risk and emergency management (Zscheischler et al., 2020). Well-documented examples include floods driven by the occurrence of intense coastal rainfall and maritime storms, known as compound coastal flood events (Sanuy et al., 2021; Romero-Martín et al., 2025), compound drought-heatwave events (Shan et al., 2024), and co-occurrence of extreme weather conditions in geographically distinct regions (Leeding et al., 2022). In the European context, the Mediterranean coast is considered a hotspot for compound events both because of their high frequency and because of the high population density and assets along the coastline (MedECC, 2024; Camus et al., 2021; Sanuy et al., 2021; Aguilera-Vidal et al., 2025; del Rosal Salido et al., 2025).

In this study, we consider three principal types of compound events. Multivariate compound events involve the simultaneous occurrence of two or more drivers and/or hazards at the same location, producing impacts greater than those generated by each driver individually. Spatially compound events arise when hazards occur simultaneously, or within a short time window, at different locations, thereby spreading impacts over a wider geographical area. Temporarily compound events consist of a sequence of drivers and/or hazards affecting the same geographical area over a relatively short period, such that recovery between events is incomplete and the cumulative impacts exceed those expected from the individual events considered in isolation.

Cascading events are a different category. A cascading hazard refers to a primary event that triggers a chain of consequences, which may range from moderate to severe (NASEM, 2022). In such cases, the "hazards" are causally linked as one or more occur because of previous hazards. For example, the interruption of railway traffic due to the collapse of a bridge over a river, or an industrial chemical spill resulting from river flooding, would both be considered cascading events. Thus, the recent fall of a wall on a train that produced one fatality on 20 January 2026 was a direct consequence of the large accumulation of water in the subsoil after an anomalous period of continuous heavy rains in Catalonia (NE Spain).

Given these characteristics, Storm Gloria provides an ideal case study for examining how different types of compound flood events can coexist within a single atmospheric episode. Previous studies have investigated the storm from several disciplinary perspectives including its hydrometeorological characteristics (SMC, 2020; OCCC, 2020; Palau et al., 2022; Iglesias et al., 2023), socio-economic and emergency-management (Llasat et al., 2023), geological, coastal, and environmental effects (González, 2020; Santasusagna Riu and Tort Donada, 2020; Canals and Miranda, 2020; Pintó et al., 2020) and marine processes, forecasting performance and coastal flooding (Amores et al., 2020; De Alfonso et al., 2021; Sotillo et al., 2021; Pérez-Gómez et al., 2021). More recently, Pantaleoni Reluy et al. (2025) adopted a multihazard perspective by integrating hazard magnitudes and economic losses, although their analysis was restricted to Catalonia. Despite these important contributions, no previous study has examined Storm Gloria as a multi-type compound event by integrating the evolution of hazards and impacts across the entire Spanish Mediterranean coast (more than 1,600 km of coastline) within an explicit compound-events framework.

In this context, the present study analyses the evolution and impacts of Storm Gloria as a compound flood event affecting the western Mediterranean coast of the IP. Within the overall episode, the three proposed types of compound events will be analysed together with cascading sequences. The remainder of this paper is organised as follows. Section 2 describes the study area and the datasets used. Section 3 outlines the methodology. Section 4 presents the temporal evolution of the storm and its associated hazards. Section 5 illustrates the different types of compound flood events identified during Storm Gloria. Section 6 analyses the interactions among the different hazards and their socio-economic consequences, and Section 7 presents the conclusions.

2 Study area and data sources

2.1 Study area

The geographical area of this study comprises the following provinces of the peninsular Spanish Mediterranean coast (Fig. 1): Girona, Barcelona and Tarragona in Catalonia (CAT); Castellón, Valencia and Alicante in the Valencian Community (CVAL); the Region of Murcia (MU) and Almería, Granada and Málaga in Andalusia (AND). Together, these ten provinces account for 83,239 km^2, about 16% of the Spanish peninsular land area, and concentrate 39% of its population (17.2 million inhabitants). The coastal strip itself includes 174 municipalities distributed along 1,609 km of coastline and covers 12,167 km^2 (approximately 15% of the total area of the ten provinces), hosting 48% of their population. This underlines the high population concentration in coastal areas (Table 1).

Table 1: Characteristics of the study region, both for the provinces as a whole and only for the coastal part: area (km²), population (2022), number of municipalities (N mun.) and number of littoral municipalities (N lit.mun.). The GDP per capita at the provincial level in EUR$_{2022}$ is also indicated, as is the value at the Spanish level.

		Provinces				Coastal municipalities		
Autonomous Community	*Provinces*	*Area (km^2)*	*Population (2022)*	*GDP/capita (EUR$_{2022}$)*	*N mun.*	*N lit. mun.*	*Area (km^2)*	*Population (2022)*
Catalonia	Girona	5,910	793,478	32,829	221	22	662	253,166
	Barcelona	7,728	5,727,615	33,369	311	27	474	2,637,967

	Tarragona	6,303	830,075	32,150	184	21	1,009	434,519
Valencian Community	Castellón	6,632	590,616	29,198	135	16	919	375,642
	Valencia	10,806	2,605,757	26,009	266	24	707	1,164,545
	Alicante	5,817	1,901,594	21,622	141	19	1,658	1,124,539
Murcia Region	Murcia	11,313	1,531,878	24,334	45	8	2,946	483,769
Andalusia	Almería	8,775	740,534	21,999	103	13	1,959	519,445
	Granada	12,647	921,987	20,349	174	10	448	116,824
	Málaga	7,308	1,717,504	21,444	103	14	1,385	1,326,398
TOTAL		**83,239**	**17,361,038**	**28,748 (Spain)**	**1,683**	**174**	**12,167**	**8,436,814**

The Spanish Mediterranean region of the Iberian Peninsula is characterised by the presence of mountain ranges running roughly parallel to the coastline. These include the *Cordilleras* Litoral and Prelitoral in Catalonia, the *Sistema Ibérico* in the Valencian Community, and the *Sistema Bético* in Murcia and Mediterranean Andalusia (Fig. 1). In some areas, such as the Valencian Community, these mountain systems extend almost directly to the coast, resulting in narrow coastal plains. The region's hydrographic network is dominated by a high density of ephemeral and torrential watercourses (locally known as "*rieres*" or "ramblas"), which respond rapidly to intense rainfall.

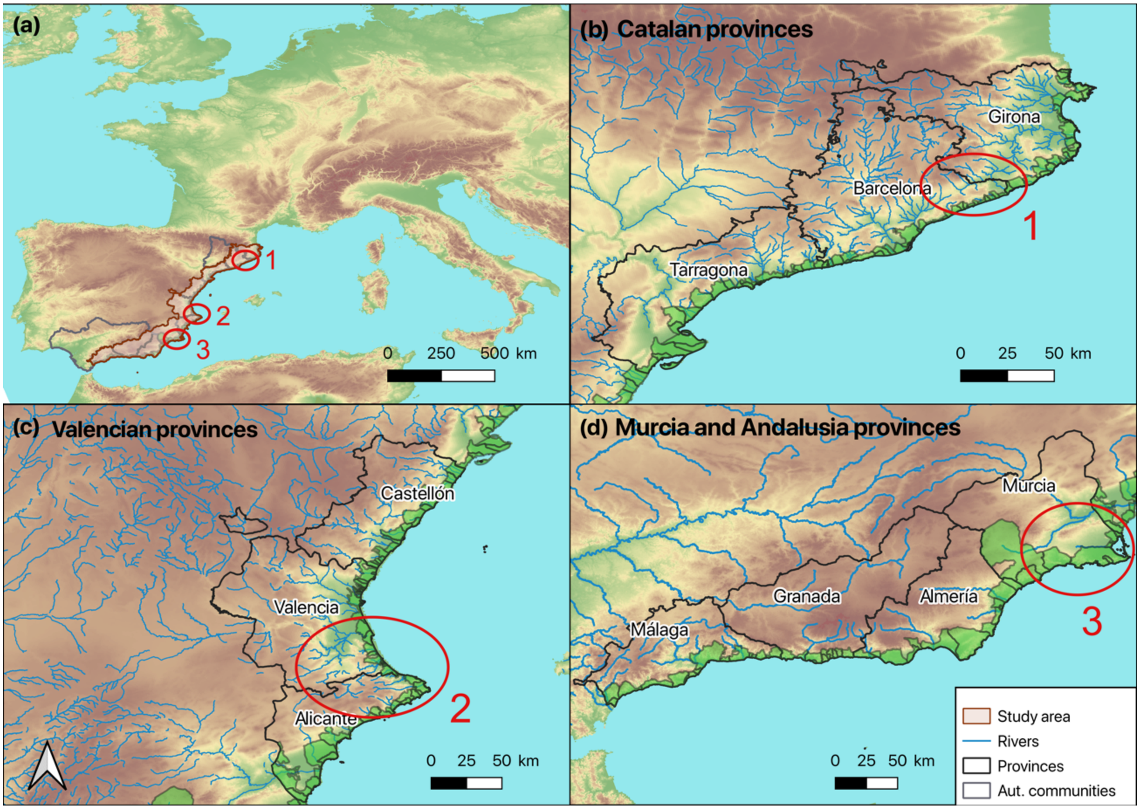

Figure 1: Localisation and main geographical features of the study area (a) and the provinces in the autonomous communities (b, c and d). Coastal municipalities are shaded in green. Locations of the three compound types of events are shown: multivariate in the Tordera River mouth (1); spatially compounding on the coast of Valencia (2); and temporally compound in Los Alcázares (3).

The most important economic sectors are tourism and construction, both of which contribute to strong urban pressure along the coast (CGRD, 2019). Other relevant sectors are agriculture (for example, intensive greenhouse cultivation in Almería), industry and logistics (particularly around Valencia and Tarragona), and major business and innovation hubs (notably in Barcelona). A clear territorial gradient in GDP per capita is observed along the peninsular Spanish Mediterranean coast: values exceed the national average in the northern provinces (Barcelona, Girona, Tarragona, and Castellón) but tend to decrease towards the south. This decline begins in Valencia, where GDP per capita already falls below the national average.

2.2 Data sources

To analyse and quantify the precipitation and wind conditions during the period from 19 to 25 January 2020, observational data were obtained from automatic weather stations operated by the Spanish Meteorological Agency (AEMET, *Agencia Estatal de Meteorología*) within the study area. For precipitation, daily accumulated rainfall

(P24h) was collected from 662 stations. For wind, maximum daily wind gusts were analysed using data from 140 automatic stations. Wave conditions were characterized using two complementary datasets. The first consisted of hourly significant wave heigh (Hs) time series from the SIMAR wave reanalysis produced by *Puertos del Estado* (http://www.puertos.es/es-es/oceanografia), extracted at 50 nodes distributed along the Spanish Mediterranean coast. For the spatial analysis, each SIMAR node was associated with its nearest coastal municipalities. To estimate the probability of multivariate and spatially compound events, Hs time series from the CoExMed wave reanalysis (Toomey et al., 2022) were used at two offshore locations near Tordera (Barcelona) and Jávea (Alicante). Unlike SIMAR, CoExMed provides a long-term wave hindcast (1950-2021) generated using a consistent modelling framework (i.e. same wave model, computational grid, and atmospheric forcing throughout the entire period), making it more suitable for statistical analysis of extremes. However, it should be noted that CoExMed systematically underestimates storm wave heights relative to SIMAR.

To identify the impacts and phenomena associated with the episode, a wide range of official sources were consulted, including official reports, press releases, government decrees, and technical studies, as well as newspaper archives (e.g. La Vanguardia, MyNews, EFE Prensa, and regional and local newspapers). Social media platforms and specialised weather websites managed by meteorology enthusiasts were used only as complementary sources to support the reconstruction of the event.

To assess the economic impact, data provided by the Insurance Compensation Consortium (CCS) were used. These data include compensation payments associated with extraordinary flooding, coastal flooding (wave-driven coastal flooding), and atypical cyclonic storms (TCA). This latter term is used by the CCS to encompass all phenomena of atmospheric origin that have caused economic damage and does not refer to either flooding or coastal flooding. It mainly includes windstorms, and tornadoes. In this article, it refers exclusively to events involving wind gusts above 120 km h^{-1}.

3 Methodology

3.1 Event definition and threshold selection

Figure 2 shows the atmospheric configuration at the surface and at 500 hPa (a, c, e) and the mean wind velocity (b, d, f), respectively, on the central days of the episode. On January 17, 2020, AEMET identified a small upper-level vortex in the North Atlantic as "Gloria." This vortex moved rapidly north of the Iberian Peninsula, where it developed into a small surface low-pressure system (AEMET, 2020b). On the afternoon of January 18, it moved into the Mediterranean, strengthening and becoming centered over the southern Balearic Islands, east of the Spanish mainland coast on January 19. On the 20th, Storm Gloria was absorbed by a larger low-pressure system located in north Africa (Fig. 2a). That didn't stop the entire episode, up to the 25th, from being known as Gloria Storm. The powerful anticyclone centered over the British Isles, with a pressure near 1050 hPa, and the low-pressure system resulted in a northward-directed pressure gradient of more than 40 hPa in less than 1500 km, which explains the strong easterly winds (gusts above 100 km/h) that produced the rough seas and the continuous influx of moist Mediterranean air in low levels (Fig. 2d). In addition to the strong winds and associated waves, precipitation was persistent and intense in eastern Spain. Snow fell at very low elevations (down to 300 meters in some areas). Due to the arrival of a very cold air mass in the preceding days, located over the Iberian Peninsula, snowfall continued at very low elevations (even down to 300 meters).

The cold upper-level disturbance enhanced instability and ascent, while the low-level flow encountered coastal mountain ranges, especially from Valencia to Catalonia, that triggered intense orographic precipitation. As seen in Figure 2, the strong anticyclone and the Mediterranean low formed a Rex Block system (a stagnant atmospheric pattern where a high-pressure system sits directly north of a low-pressure system). This type of weather is characterized by its ability to remain unchanged for days or even weeks. Figure 2b shows the strong easterly winds that advected very warm and humid air over the coast.

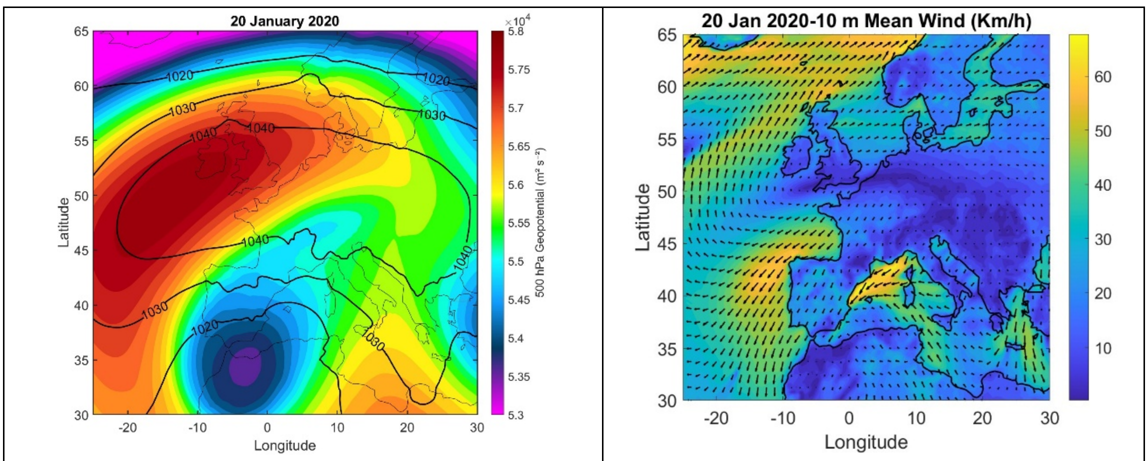

(a) (b)

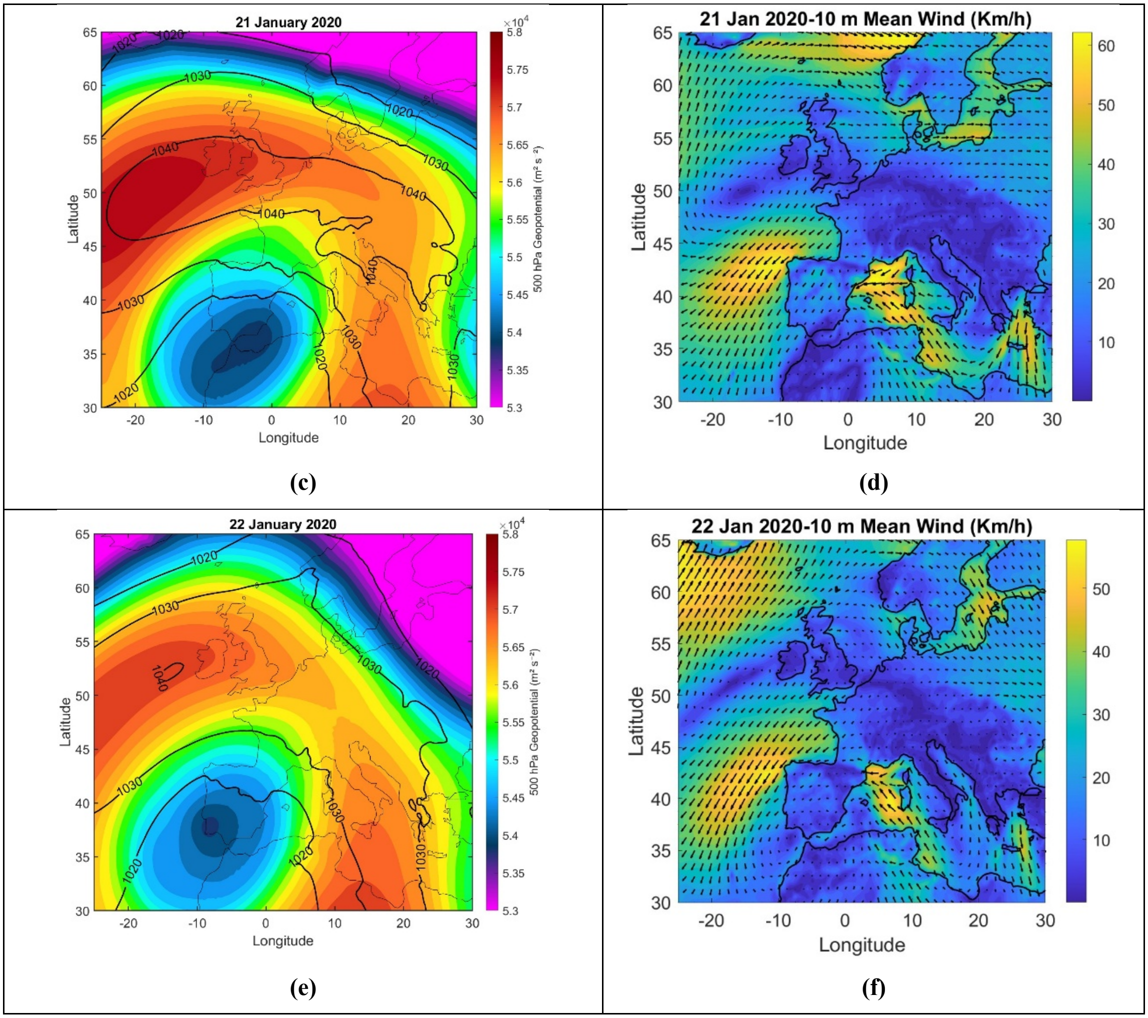

Figure 2: Sea level pressure and 500 hPa geopotential (a, c, e) and mean wind speed (b, d, f) for January 20, 21 and 22, 2020.

The initial and final dates of the event were first identified from previous reports and analyses (SMC, 2020; González, 2020; AEMET, 2020a, b). However, discrepancies were noted among the different sources regarding the exact temporal limits of the episode. To ensure consistency, the event window used in this paper was defined objectively as the period during which daily precipitation exceeded 40 mm in at least two stations within the study area. Under this criterion, the Gloria event lasted from 19 to 25 January 2020. This definition was further supported by the synoptic reanalysis, which confirmed that the rainfall observed on 25 January was associated with the same meteorological system and should therefore be considered part of the event.

To characterise the event from a meteorological perspective, the observations recorded between 19 and 25 January 2020 were classified into three severity categories based on previous studies and on operational thresholds used by AEMET and SMC (*Servei Meteorològic de Catalunya* or Meteorological Service of Catalonia) (Table 2). This framework allows moderate, significant, and extreme values to be distinguished consistently across the study area.

For 24 h precipitation (P24h), thresholds of 40, 100, and 200 mm were adopted. The minimum threshold of 40 mm has been widely used in studies of intense rainfall and flooding in the Mediterranean region (Cortès et al., 2019; Sanuy et al., 2021), while the 100 and 200 mm thresholds are also commonly used as operational reference levels for heavy-rainfall warnings in the study region. For maximum wind gusts, thresholds of about 70, 90, and 100 km h^{-1} were selected from AEMET warning criteria and previous studies (Amaro et al., 2010; Romero-Martín et al., 2024). Wave severity was characterised using the daily maximum significant wave height (Hs), computed from hourly values between 00:00 and 24:00 UTC. For spatial attribution, each SIMAR station was associated with its nearest coastal municipalities, allowing daily wave-height values to be assigned to the 174 coastal municipalities in the study area. For consistency across the whole study area, thresholds of 2, 5, and 7 m were adopted. The first threshold is consistent with storm conditions along the Catalan coast and is conservative for sectors where lower operational thresholds are sometimes used, such as 1–1.5 m in the Andalusia–Valencia sector (ROM, 1991). The higher thresholds are consistent with values commonly used in the literature to distinguish severe and extreme wave conditions (Del Río et al., 2012; Mendoza et al., 2011; Romero-Martín et al., 2024), thereby providing three robust and spatially consistent categories of wave severity.

Table 2: Hazard intensity thresholds

Category	Precipitation (24h, mm)	Max. wind gust (km h^{-1})	Wave height (daily Hs, m)
1	40	70	2
2	100	90	5
3	200	100	7

3.2 Impact assessment

To assess the damage caused by the event, the total compensation paid by the CCS for insured property was calculated for each municipality within the study area. CCS data provide a useful proxy for economic impact and have already been used in previous studies (e.g. Cortès et al., 2018; Rivas et al., 2022). Since CCS provides records at the postal code level, the data were aggregated to municipality level following the approach of Cortès et al. (2018): (1) selecting claims dated between the first day of the event and 7 days after its end, and (2) summing the selected claims within each municipality. All monetary values were converted to constant EUR_{2022} using the Consumer Price Index, unless otherwise stated.

3.3 Probabilistic analysis of selected compound sub-events

Storm Gloria was a long-lasting, spatially extensive episode involving interacting hazards such as heavy rainfall, high waves, strong winds, snowfall, hail, and local landslides. Although the episode as a whole can be described as a compound event, its internal structure can also be decomposed into different compound-event typologies. Three sub-events were selected for detailed analysis based on their representativeness, data availability, and impact relevance: a multivariate case at the Tordera mouth, a spatially compounding inland–coastal case linking the Júcar basin and the Gulf of Jávea, and a temporally compounding case associated with repeated impacts in Los Alcázares. To quantify the probability of multivariate and spatially compound events, their joint occurrence was assessed using the two-sided conditional framework proposed by Wahl et al. (2015). Two event types were defined: (i) wave-dominated events, denoted ($Hs_{CoExMed}$_99.5, P24h), in which an extreme $Hs_{CoExMed}$ event was paired with the maximum concurrent P24h within the selected subregion; and (ii) rainfall-dominated events, denoted (P24h, $Hs_{CoExMed}$), in which an extreme P24h event was paired with the highest co-occurring $Hs_{CoExMed}$. For the multivariate analysis, both variables correspond to the same location (the Tordera coastal sector and its corresponding river basin), whereas for the spatially compound analysis, wave conditions were represented by the offshore node near Jávea and precipitation by the Júcar river basin.

Extremes of the conditioning variable were modelled using a peaks-over-threshold Generalised Pareto Distribution. For the paired variable, several candidate distributions (exponential, two-parameter gamma, lognormal, Weibull, and Tweedie) were fitted, with the optimal distribution selected according to the Akaike Information Criterion (AIC). The dependence structure between variables was modelled using copulas (Coles and Tawn, 1991; Coles et al., 1999; Genest and Favre, 2007), implemented through the VineCopula R package (Nagler et al., 2025). Joint return periods were then estimated by combining the two conditional bivariate models following the methodology of Wahl et al. (2015).

Although CoExMed underestimates storm Hs relative to the SIMAR reanalysis, the estimated probabilities are considered representative of Storm Gloria because the analysis assumes that this bias affects to the magnitude of wave heights but not the temporal occurrence of extreme events or their dependence with precipitation.

Finally, for the temporarily compound event case, the probability of occurrence of the observed sequence of rainfall events was estimated empirically using the available precipitation time series from the Los Alcázares area.

4 Overall characterisation and temporal evolution of Storm Gloria

4.1 Spatial distribution of maximum hazard intensity

Storm Gloria produced exceptionally widespread hydrometeorological conditions across the Spanish Mediterranean coast. During the period 19-25 January 2020 almost 90% of the analysed raingauges recorded more than 40 mm of accumulated precipitation, with 37% recording between 100 and 200 mm and 22% exceeding 200 mm. The highest totals occurred in northern Catalonia and in the Valencian Community (Fig. 3). Eleven stations, from Alicante to northern Girona, recorded more than 400 mm, reaching a maximum of 527.5 mm at L'Orxa (Alicante; Table 3). Such a large number of stations exceeding 200 mm confirms the exceptional character of the episode.

Maximum wind gusts showed a similar regional pattern, although their spatial variability was lower than that of precipitation. Nineteen AEMET stations recorded wind gusts above 90 km h^{-1} with the highest values measured in the province of Valencia (108 km h^{-1} on 19 January and 115 km h^{-1} on the 20th, respectively) (Table A1, in the Appendix). The wave field was even more spatially extensive, affecting almost the entire Mediterranean coastline. Offshore significant wave height exceeded 8 m in several locations, reaching a maximum of 8.75 m, whereas lower values were observed along the Andalusian coast owing to its south-facing orientation, which reduced exposure to the dominant easterly wave conditions. When the three hazard variables are considered jointly, clear spatial differences emerge. Valencia was the only province where precipitation, wind gusts, and wave height simultaneously reached the highest category for all three hazards, while Girona, Barcelona, Alicante, and Murcia reached the highest category for two of the three variables. Conversely, Granada experienced only low precipitation levels and comparatively weak marine forcing. These regional contrasts illustrate that, although Gloria affected the entire Spanish Mediterranean coast, the relative contribution of each hazard varied substantially alongshore. Table 6 summarises the category reached by each variable in at least two stations in the province.

The observed distribution of hazards largely reflects the interaction between the synoptic circulation and regional physiography. Maximum rainfall occurred where coastal mountain ranges lie close to the shoreline, particularly between Valencia and Catalonia, where persistent easterly winds enhanced orographic uplift. In contrast, the wave field was primarily controlled by the pressure gradient over the western Mediterranean, producing energetic sea states along almost the entire eastern Spanish coastline irrespective of local topography.

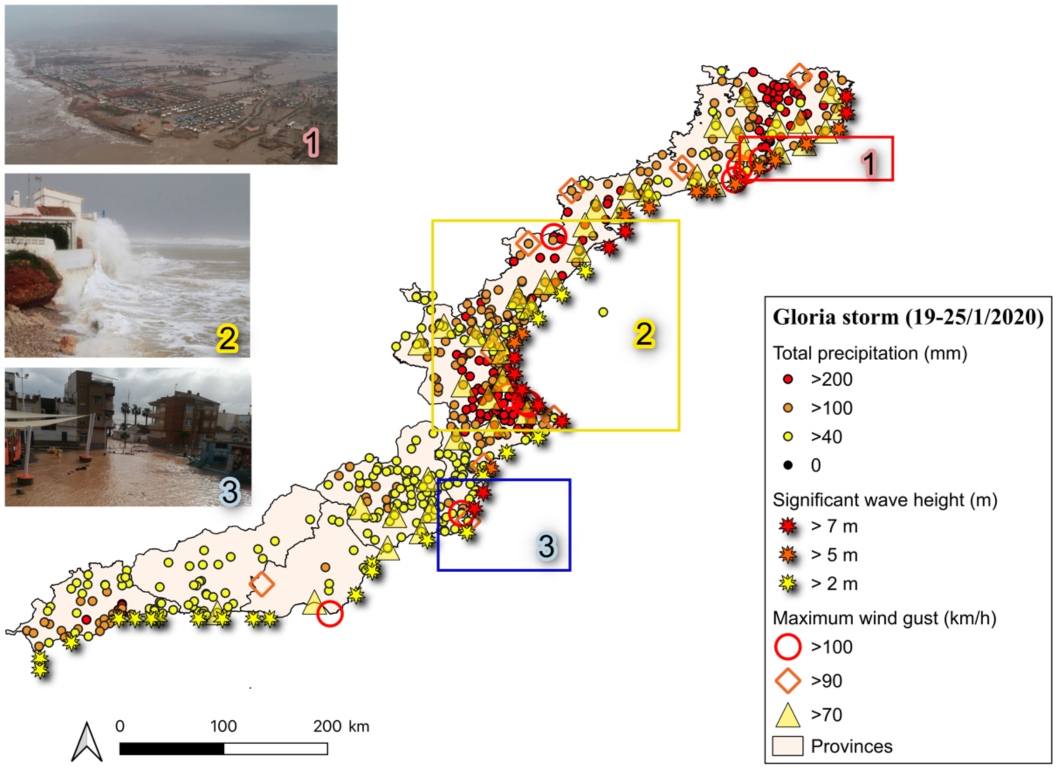

Figure 3: Map of the maximum thresholds exceeded at some point during the Gloria episode in the study area. Selected types of compound events are highlighted with boxes and photographs: (1) multivariate in the Tordera River mouth; (2) spatially compounding on the coast of Valencia; and (3) temporally compound in Los Alcázares.

Table 3: Stations that recorded a total precipitation above 400 mm. *Coordinates are in decimal degrees (WGS84; EPSG:4326)

Coordinates (lat, lon)*	**Station name** (altitude in m)	**Province**	**Ptotal** (19/1-25/1)	**P24h max** (day)
38.84º N, 0.31º W	Lorxa (in L'Orxa) (270)	Alicante	527.5	266.5 (19)
42.29º N, 2.68º E	Albanyà-Lliurona (732)	Girona	515.2	208 (21)
39.00º N, 0.29º W	Barx-la Drova (372)	Valencia	471.5	273.6 (19)
38.81º N, 0.40º W	Gaianes (454)	Alicante	432.5	220.6 (19)
39.01º N, 0.30º W	Barx (340)	Valencia	432	242 (20)
41.81º N, 2.33º E	La Morera (in El Brull) (882)	Barcelona	424.5	236 (20)

38.74º N, 0.29º W	Benimassot (725)	Alicante	423	227.5 (20)
42.14º N, 2.53º E	Santa Pau-Sacot (609)	Girona	410.4	225 (21)
41.89º N, 2.43º E	Vilanova de Sau-El Tortades (818)	Barcelona	409.2	194.5 (21)
42.12º N, 2.63º E	Mieres (271)	Girona	408.7	150.5 (22)
42.26º N, 2.36º E	Sant Pau de Segúries-La Barquera (872)	Girona	403.5	220.5 (22)

4.2 Temporal evolution

Daily precipitation, maximum wind gust and significant wave height were analysed for the whole event (19-25 January). However, after 23 January, wave heights had fallen below the adopted thresholds, so the final two days were relevant mainly for rainfall. The first day of the event, 19 January, was characterised by values above the highest threshold for all three variables (precipitation, wind gusts and wave height) in the province of Valencia. Notably, 277 mm were recorded in Barx (Valencia), accompanied by a wind gust of 108 km h^{-1}. Significant wave heights over 7 m (with a maximum of 7.67 m) were observed offshore, particularly in front of the coasts of Valencia and Alicante, including the area near Jávea.

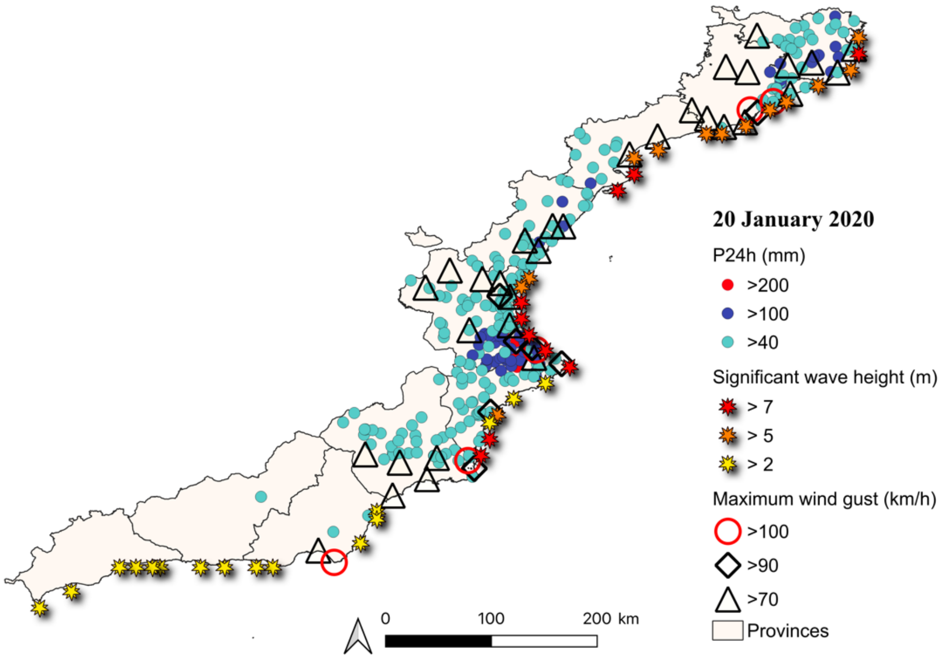

Figure 4: Stations where the significant wave height, maximum wind gusts and precipitation thresholds were exceeded on 20 January 2020. Appendix A contains maps for the other days of the event.

The storm reached its maximum intensity and geographical extent on 20 January. The heaviest rainfall was again recorded in the provinces of Valencia and Alicante, with peaks of 242 mm in Barx and Xàtiva (Fig. 4). Wind gusts were more widespread and slightly stronger than the previous day, reaching a maximum of 115 km h^{-1} in Oliva (Valencia), followed by 104 km h^{-1} in San Javier (Murcia) and 103 km h^{-1} in the Fabra Observatory (Barcelona) and Cabo de Gata (Almería). Wave heights remained high, with the most extreme values again concentrated off the coasts of Valencia and Alicante, and locally in Girona and Tarragona. The highest recorded significant wave height was 10.1 m offshore from Jávea. On the 21st, the focus of maximum intensity shifted to the provinces of Barcelona and Girona, which recorded the highest across all three variables. Precipitation exceeded 200 mm at several locations, with a peak of 236 mm in El Brull (Barcelona). The maximum wind gust was 106 km h^{-1}, recorded at the Barcelona AEMET station. Significant wave heights above 5 m were observed along the Catalan coast, particularly in Barcelona and Girona, with a maximum of 7.46 m in the northern coastal sector of Girona. On the 22nd, the intensity decreased compared to the previous day. Nevertheless, medium-level thresholds (level 2) were exceeded simultaneously for all three variables in the province of Girona, with the highest wave values still concentrated along the Catalan coast.

On the 23rd, the most notable rainfall occurred in the province of Málaga, with 202 mm recorded in Coín. Although heavy rainfall persisted in Málaga on 24 and 25 January, exceeding 100 mm on both days, no significant wind gusts or wave heights were recorded during this final phase of the event.

5 Analysis of the Selected Compound Events

Storm Gloria generated multiple types of compound flood events that developed simultaneously across the Spanish Mediterranean coast. To illustrate the diversity of mechanisms involved, three representative examples are analysed, corresponding to multivariate, spatially compound and temporarily compound events (Table 4). Together, these case studies demonstrate how different combinations of hazard drivers produced distinct impact pathways and management challenges during a single atmospheric episode. In addition, the event generated cascading impacts, such as the collapse of the Tordera bridges, and was influenced by preconditioning factors, including antecedent beach erosion, which further amplified storm impacts.

Table 4: Main characteristics of the selected types of compound events

Type	Description	Selected data	Return period
Multivariate	Simultaneous heavy precipitation in the Tordera River basin + High waves in the river mouth.	Weather stations in the Tordera River basin and waves (SIMAR and CoExMed) nodes in front of the mouth of the Tordera River.	85 years
Spatially compounding	High waves off the Jávea coast (Alicante) concurrent with heavy rainfall and flooding in the Júcar river basin (Valencia).	Weather stations in the Júcar River basin and waves (SIMAR and CoExMed) node in front of Jávea.	72 years
Temporally compounding	Three consecutive flood events between 11 September 2019 and 25 January 2020 in Los Alcázares (Murcia).	Weather stations in the Segura River basin and surrounding municipalities.	22 years

5.1 Multivariate event: flooding of the Tordera delta

5.1.1 Event description

The flooding of the Tordera delta (Barcelona) provides a representative example of a multivariate compound flood, in which fluvial and coastal processes interact simultaneously at the same location (Fig. 3). During Storm Gloria, intense rainfall over the Tordera River basin generated exceptionally high river discharge, while energetic wave conditions at the river mouth impeded drainage to the sea. The resulting backwater effect increased water levels within the lower river reach and enhanced flooding across the delta plain. At the same time, wave overtopping contributed to inundation of the seaward part of the delta, further increasing flood extent. The severity of the event was enhanced by the geomorphological evolution of the delta. The Tordera coastline has undergone persistent shoreline retreat as a consequence of reduced sediment supply, resulting in progressive erosion of the beach system (Jiménez et al., 2018). This loss of the natural coastal buffer has increased the exposure of low-lying areas to marine flooding during severe storms. Consequently, the Tordera delta has been identified as one of the principal hotspots of compound flooding along the Catalan coast (Sanuy et al., 2021). Exposure within the delta is also particularly high owing to the presence of transport infrastructure, agricultural land and numerous campsites located immediately behind the beach. Although campsite occupancy peaks during summer, when the probability of severe storms is comparatively low (Sanuy and Jiménez, 2021; Aguilera-Vidal et al., 2025), their location within low-lying flood-prone areas makes them particularly vulnerable to compound flooding. One of the most significant consequences of the event was the collapse of the railway bridge crossing the Tordera River after one of its piers was undermined by the flood flow. The subsequent failure of the adjacent road bridge produced major disruption to regional transport (González, 2020), illustrating how a compound flood can trigger cascading failures in interconnected infrastructure systems.

5.1.2 Probabilistic characterization

The probability of occurrence of this compound event was evaluated using P24h recorded at meteorological stations within the Tordera river basin and Hs from the offshore CoExMed node located seaward of the river mouth (Fig. 5), representing the fluvial and marine drivers, respectively.

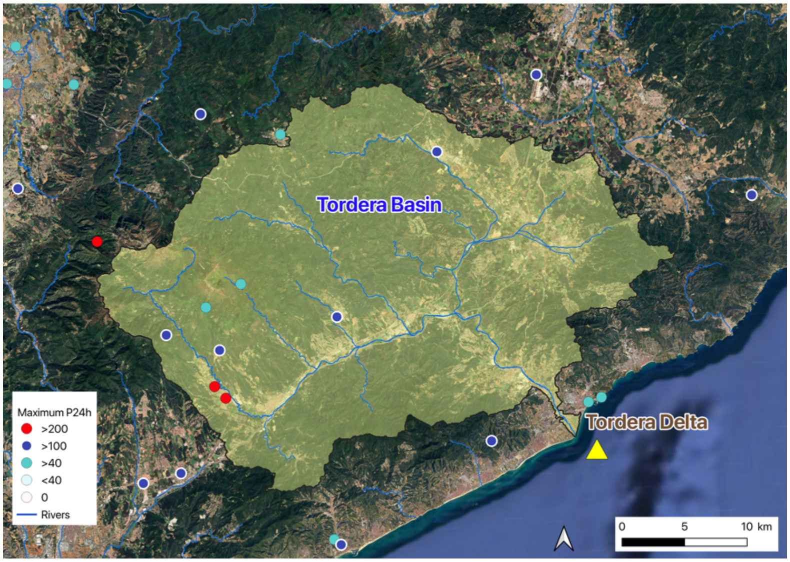

Figure 5: AEMET AWS (operative automatic weather stations) in the Tordera River basin and surrounding areas, and CoExMed wave node off the river mouth (yellow triangle). The stations are coloured according to the maximum recorded P24h value following the criteria described in 3.1 (Map data © 2025 Google).

During Storm Gloria, the maximum precipitation recorded within the basin reached 225 mm, while offshore Hs attained 4.5 m, equivalent to approximately 5.9 m in the SIMAR reanalysis. Considered independently, these values correspond to return periods of approximately 24 years for precipitation and 60 years for wave height. Assuming statistical independence between both drivers, their simultaneous occurrence would therefore correspond to an estimated return period of approximately 1,440 years. Copula modelling, however, revealed a positive dependence between rainfall and wave extremes. Rainfall-conditioned events were best represented by a survival BB7 copula (Kendall's $\tau = 0.20$), whereas wave-conditioned events followed a Tawn Type I copula with a similar degree of dependence. Accounting for this dependence substantially increased the likelihood of joint occurrence, reducing the estimated return period from 1,440 years to approximately 85 years (Fig. 6). This result demonstrates the importance of explicitly considering dependence between flood-generating processes, as assuming independence would considerably overestimate the rarity of the event.

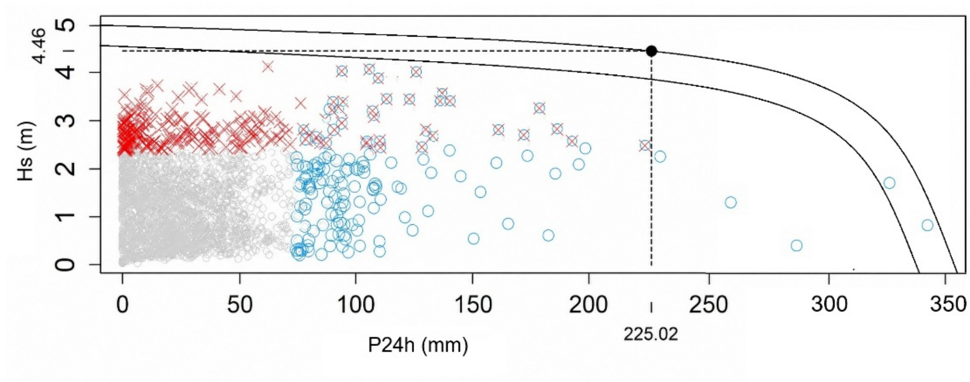

Figure 6: Estimated joint return period of the Gloria storm at the Tordera River mouth. Red crosses denote events with Hs exceeding the local storm threshold, blue circles denote events with P24 exceeding the local precipitation threshold, and grey symbols represent non-extreme conditions. The overlap of red crosses and blue circles denotes compound extreme events. Curves indicate joint return periods of 50 years (inner curve) and 85 years (outer curve), the latter corresponding to Storm Gloria (black filled circle).

5.1.3 Implications

Beyond its statistical rarity, the Tordera case illustrates the distinctive characteristics of multivariate compound flooding. The interaction between fluvial discharge and coastal processes generated impacts considerably greater than those expected from either driver acting in isolation. Moreover, the concentration of critical infrastructure, tourism facilities, and agricultural land within the delta transformed a hydrometeorological event into a complex societal disruption. The collapse of the road and railway bridges demonstrates how multivariate compound events may initiate cascading failures that propagate well beyond the directly flooded area. Recovery was further complicated by the involvement of multiple administrative authorities responsible for transport infrastructure, coastal management, and flood protection. Six years after the storm, adaptation measures combining nature-based solutions, shoreline restoration, land-use planning, and structural interventions are still being implemented within the Tordera delta, illustrating the long-term challenges associated with recovering from compound flood disasters.

5.2 Spatially compounding event: heavy rainfall in the Júcar basin and severe wave conditions along the Jávea coast

5.2.1 Event description

This case illustrates a spatially compound flood event, in which the principal flood-generating hazards occurred simultaneously but at geographically distinct locations (Fig. 3). During Storm Gloria, intense rainfall affected the Júcar River basin, generating widespread pluvial and fluvial flooding, while exceptional wave conditions developed along the Gulf of Jávea, producing severe coastal flooding and erosion. Although these hazards were hydrologically independent, their concurrent occurrence substantially increased the complexity of emergency response and recovery. The example presented here is representative of a much broader regional pattern. Throughout the storm, heavy rainfall and energetic wave conditions affected multiple sectors of the Valencian Community simultaneously. The region covers approximately 23,300 km^2, includes more than 470 km of densely urbanised coastline, and is crossed by numerous torrential rivers and ephemeral streams. Consequently, emergency management authorities were required to respond simultaneously to inland flooding, coastal inundation, infrastructure damage, and transport disruption occurring at different locations but within the same administrative jurisdiction.

Along the Jávea coastline, significant wave heights reached between 7 and 10 m, producing widespread damage to beaches, promenades, ports, and seafront properties. At the same time, heavy rainfall within the Júcar basin caused extensive pluvial and fluvial flooding, resulting in road closures, transport disruption, and temporary airport operational restrictions. Unlike the multivariate event described for the Tordera delta, the principal challenge here did not arise from the interaction of hazards at the same location but from their simultaneous occurrence across a large geographical area, which substantially complicated emergency coordination and resource allocation.

5.2.2 Probabilistic characterization

The probability of occurrence of this spatially compound event was estimated using P24h recorded within the Júcar river basin together with Hs from the CoExMed node located in the Gulf of Jávea (Fig. 7), representing the fluvial and marine drivers, respectively.

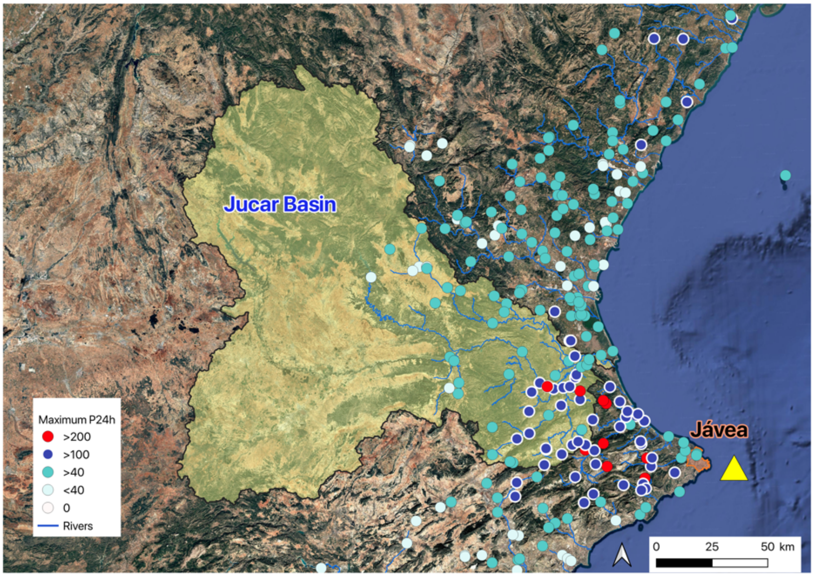

Figure 7: Location of the AEMET AWS (automatic weather stations) inside the Júcar River basin and surrounding area, and the node CoExMed located in the Gulf of Jávea (yellow triangle). The stations are coloured according to the maximum recorded P24h value following the criteria described in 3.1 (Map data © 2025 Google).

During Storm Gloria, maximum daily precipitation within the basin reached 274 mm, whereas Hs attained 7 m (equivalent to approximately 10 m in the SIMAR reanalysis). Considered independently, these values correspond to return periods of approximately 1.5 years for precipitation and 100 years for wave height. Assuming statistical independence, the simultaneous occurrence of both extremes would therefore correspond to a return period of approximately 150 years. Copula analysis identified a positive dependence between rainfall and wave extremes. Rainfall-conditioned events were best represented by a survival Tawn Type II copula (Kendall's $\tau = 0.12$), whereas wave-conditioned events followed a Tawn Type I copula with a similar dependence structure. Accounting for this dependence reduced the estimated joint return period from approximately 150 years to 72 years (Fig. 8). Although the dependence between both drivers is weaker than in the multivariate Tordera case, it still substantially increases the probability of joint occurrence. This result illustrates that even relatively modest statistical dependence can significantly influence estimates of the likelihood of spatially compound flood events.

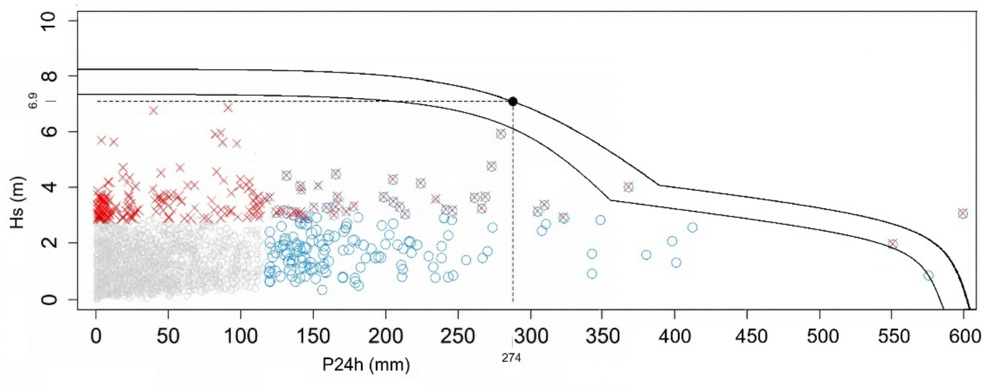

Figure 8: Estimated joint return period of the Gloria storm at the Júcar river basin and the Jávea coast. Red crosses denote events with Hs exceeding the storm threshold at Jávea, blue circles denote events with P24 exceeding the precipitation threshold at the Júcar river basin, and grey symbols represent non-extreme conditions. The overlap of red crosses and blue circles denotes compound extreme events. Curves indicate joint return periods of 50 years (inner curve) and 72 years (outer curve), the latter corresponding to Storm Gloria (black filled circle).

5.2.3 Implications

Unlike multivariate compound floods, whose impacts arise from the physical interaction of coincident hazard drivers, spatially compound events primarily increase the complexity of emergency management. Simultaneous flooding at multiple locations forces emergency services to distribute personnel, equipment, and logistical resources across large geographical areas, reducing operational flexibility and increasing the potential for resource shortages. Storm Gloria clearly illustrates these challenges. During the peak of the event, inland flooding, coastal inundation, infrastructure damage, and transport disruption occurred simultaneously throughout the Valencian Community, requiring coordinated response by a single regional authority across widely separated locations. This type of event therefore places exceptional demands on emergency planning, interagency coordination, and resource allocation. More broadly, the case demonstrates that the severity of spatially compound events depends not only on the magnitude of individual hazards but also on their geographical footprint. As recently shown for the Spanish Mediterranean coast by Aguilera-Vidal et al. (2026), certain atmospheric circulation patterns promote strong spatial connectivity between rainfall and coastal storms, increasing the probability that multiple flood emergencies will occur simultaneously over large regions. Consequently, incorporating spatial connectivity into hazard assessments is essential for realistic emergency planning and regional flood-risk management.

5.3 Temporally compounding event: successive flood episodes in Los Alcázares

5.3.1 Event description

The flooding of Los Alcázares (Murcia) illustrates a temporally compound flood event, in which the impacts of Storm Gloria were amplified by the occurrence of previous damaging floods before recovery had been completed (Fig. 3). Unlike the multivariate and spatially compound examples presented above, the defining characteristic of this event is therefore not the magnitude of any individual storm but the clustering of damaging events before recovery from previous floods had been completed. Los Alcázares is located on the western shore of the Mar Menor, within the lower Segura River basin (Fig. 9). The municipality is intersected by several ephemeral channels, including the Rambla del Albujón and the Rambla de la Maraña, which produce a diffuse flood response as runoff reaches the urban area through multiple drainage pathways. Extensive urban development within flood-prone areas, together with the modification of natural drainage channels and the presence of transport and utility infrastructure across flow paths, has substantially increased both exposure and flood vulnerability (MITECO, 2020).

Figure 9: Map of the municipality of Los Alcázares and neighbouring municipalities in Murcia mentioned in the text, showing rivers and the location of AEMET AWS (automatic weather stations). The stations are coloured according to the maximum recorded P24h value during the Storm Gloria 2020 following the criteria described in 3.1 (Map data © 2025 Google).

The first event in the sequence occurred between 11 and 15 September 2019, when exceptionally intense rainfall generated widespread flooding throughout the Segura basin. Maximum P24h reached 321 mm in San Javier and 257 mm in Molina de Segura (Northwest of San Javier, 35 km from the sea) causing extensive damage to buildings, public infrastructure, and municipal services in Los Alcázares (Fig. 10). The severity of the event led the municipality to be officially declared an “area seriously affected by a civil protection emergency”. For this episode alone, the CCS paid more than EUR2022 24 million in Los Alcázares, accounting for 74% of the total compensation disbursed in the municipality between 1996 and 2020.

Approximately three months later, on 2-3 December 2019, a second heavy-rainfall episode affected the basin. Although less intense than the September event, with a maximum P24h of 145 mm (while San Javier registered 115 mm in 24 hours), it caused renewed flooding while recovery operations from the previous disaster were still underway. Roads were inundated, around one hundred residents were evacuated, and infrastructure that had only partially been repaired suffered additional damage.

Storm Gloria constituted the third event in the sequence. On 20-21 January 2020, maximum P24h again reached approximately 145 mm within the Segura basin. Although the direct physical damage was less severe than that produced by the September flood, the social consequences were substantially greater because the municipality had not yet recovered from the previous two events. The repeated occurrence of flooding generated widespread public dissatisfaction and culminated in a large demonstration in Los Alcázares on 26 January 2020 demanding more effective mitigation measures.

Taken together, these three events exemplify the concept of a temporally compounding. The severity of the January 2020 disaster resulted not only from the meteorological conditions associated with Storm Gloria but also the persistence of physical damage, accumulated economic losses, and declining social resilience following the preceding floods.

(a) (b)

Figure 10: Floods in Los Alcázares: (a) September 2019, during the DANA event (source: Confederación Hidrográfica del Segura); and (b) January 2020 (source: Government of the Region of Murcia).

5.3.2 Probabilistic characterization

The probability of this temporally compound event was estimated using daily precipitation records from the Segura River basin, which were considered representative of the regional hydrometeorological forcing responsible for the repeated flooding of Los Alcázares (Fig. 9). Consequently, the estimated return period refers to the recurrence of a sequence of basin-scale rainfall extremes rather than to flood losses in the municipality itself. During Storm Gloria, maximum P24h reached 145 mm within the basin. This event occurred under exceptionally wet antecedent conditions, with accumulated precipitation of 115 mm during the preceding month and 257 mm over the previous three months, indicating that Gloria formed part of an unusually persistent period of heavy rainfall. The defining characteristic of this case is therefore not the magnitude of an individual storm but the temporal clustering of successive extremes (e.g. Haigh et al., 2016). Within less than five months, the basin experienced three major rainfall episodes, one exceeding 300 mm and two exceeding 140 mm in 24 hours. A comparable sequence occurred only twice during the available 43-year observational record, corresponding to an empirical return period of approximately 22 years. Although this estimate provides a useful indication of the rarity of the event sequence, it should be interpreted with caution because of the limited length of the observational record and the uncertainty associated with estimating the recurrence of clustered extreme events from empirical observations alone.

5.3.3 Implications

The Los Alcázares case demonstrates that the impacts of compound events depend not only on hazard magnitude but also on recovery dynamics. Although the January 2020 flood was considerably less severe than the September 2019 event from a hydrometeorological perspective, its occurrence before complete recovery had been achieved substantially amplified its societal consequences. This amplification operated through several mechanisms. Physically, previously damaged infrastructure remained more vulnerable to subsequent flooding. Economically, repeated losses imposed an increasing burden on households, businesses, and public administrations. Socially, the succession of disasters progressively reduced community resilience and increased public dissatisfaction regarding flood management and recovery measures. Consequently, the disaster was defined not by the intensity of the final event alone but by the cumulative effects of the entire event sequence.

The case also highlights an aspect that is frequently overlooked in conventional flood-risk assessments. Return periods are generally calculated for individual events, implicitly assuming that each event occurs under independent antecedent conditions. However, when recovery times exceed the interval between successive extremes, disaster severity becomes strongly conditioned by event sequencing rather than by the magnitude of any single event (de Ruiter et al., 2020). Recovery time should therefore be regarded as an integral component of compound flood risk assessment, particularly in regions where climate change is expected to increase the frequency of extreme precipitation events and reduce the time available for recovery.

Taken together, the three case studies illustrate that compound flood events differ not only in their physical mechanisms but also in the scales at which they operate and in the management challenges they generate. Multivariate events amplify hazard intensity through the interaction of coincident drivers, spatially compound events increase the complexity of emergency response by simultaneously affecting multiple locations, and temporally compound events amplify impacts through incomplete recovery between successive disasters. Storm Gloria demonstrates that all three mechanisms may coexist within a single atmospheric episode, producing a level of societal disruption that cannot be understood from any individual event type alone.

6 Main impacts and economic losses

6.1 Societal and environmental impacts

Storm Gloria produced widespread disruption throughout the Spanish Mediterranean coast. According to CCS records, 770 municipalities were affected, representing 46% of all municipalities within the analysed provinces and 82% of those located along the coast (Table 5). The event resulted in ten confirmed fatalities in the study region: four deaths (two in a car swept away by floodwaters, two by waves) and one missing person in Catalonia; five deaths in the Valencian Community (two homeless people swept away by floodwaters while sleeping and another one from hypothermia, and two from unknown causes); and one death in Andalusia. Across all of Spain, Storm Gloria resulted in 14 deaths and three missing persons.

Table 5: Number of municipalities affected by flooding, coastal flooding, and TCA (Atypical Cyclonic Storms), following the CCS classification, by coastal provinces in every autonomous community and for the study area as a whole. *In the total figure for each region, each municipality is counted only once, even if it has been affected by one, two or three hazards. The total number of municipalities in each province is provided in Appendix A.

	Catalan	Valencian	Murcia	Andalucia	Total

	prov.	prov.	prov.	prov.	
Floods	422	224	15	31	692
Coastal floods	55	45	2	0	102
TCA	194	56	4	2	256
Total*	474	249	15	32	770

The storm affected virtually every socioeconomic sector. Along the coast, the most severe impacts occurred in Catalonia and the Valencian Community, where extensive beach erosion, coastal flooding, and substantial damage to promenades, ports, marinas, and other coastal infrastructure were reported. Inland, the overflow of rivers and ephemeral streams caused widespread flooding of residential areas, commercial premises, industrial facilities, hotels, and thousands of vehicles. Strong winds also damaged buildings, urban furniture, and public infrastructure, particularly within the Barcelona metropolitan area.

Transport infrastructure was severely disrupted throughout the region. Numerous roads and railway lines were closed because of flooding, landslides, fallen trees, and snow accumulation. Particularly significant was the collapse of the railway and adjacent road bridges across the Tordera River, which interrupted one of the principal transport corridors along the Catalan coast. Rail services were not fully restored for approximately ten months. Airport operations in the Valencian Community and Andalusia were also temporarily affected.

Primary economic activities sustained substantial losses. Agricultural damage was particularly severe in the Ebro Delta, where extensive rice fields were flooded, and in Níjar (Almería), where numerous greenhouses were damaged. The Union of Small Farmers and Ranchers estimated agricultural losses throughout Spain at approximately EUR2022 24.1 million. Fishing activity ceased during the storm and remained interrupted for more than a week owing to the large quantities of sediment and debris transported to the coast by rivers. Additional losses resulted from damage to fishing vessels, gear, and offshore tuna-fattening facilities near l'Ametlla de Mar (Tarragona), where thousands of fish died.

From an ecological perspective, the storm had substantial impacts on several natural environments, including the Ebro Delta (Catalonia) and l’Albufera of Valencia. Particularly severe damage was reported in *Posidonia oceanica* meadows, which were strongly affected by the marine storm, while intense winds also caused widespread tree uprooting (Marco-Méndez et al., 2024). At the same time, some positive effects were identified, such as the regeneration of the Tordera delta through sediment input and the recharge of aquifers and reservoirs. Daily life was also seriously disrupted, with school closures, interruptions to electricity and drinking water supply, and damage to collectors, water treatment plants, and sewage systems in multiple localities. Beyond these direct effects, the event generated significant indirect impacts, including travel delays and the temporary suspension of economic activity. Intangible damage should likewise be acknowledged, following the classifications proposed by Petrucci and Llasat (2013) and Messner and Meyer (2006), particularly anxiety and stress among affected populations.

6.2 Economic compensation

The total amount of compensation paid across the study area reached EUR_{2022} 204 million, of which EUR_{2022} 106.5 million was associated with flooding, EUR_{2022} 40.3 million with coastal flooding, and EUR_{2022} 57.2 million with windstorms (TCA following the nomenclature of CCS). Figure 11 shows the distribution of these payments by hazard type: 52% corresponded to floods, 28% to TCA, and 20% to coastal flooding. However, restricting the analysis to coastal municipalities substantially changes this distribution. In these municipalities, flooding represented 43% of total compensation, whereas coastal flooding and wind-related claims each accounted for 29%, highlighting the increasing economic importance of marine hazards in coastal environments.

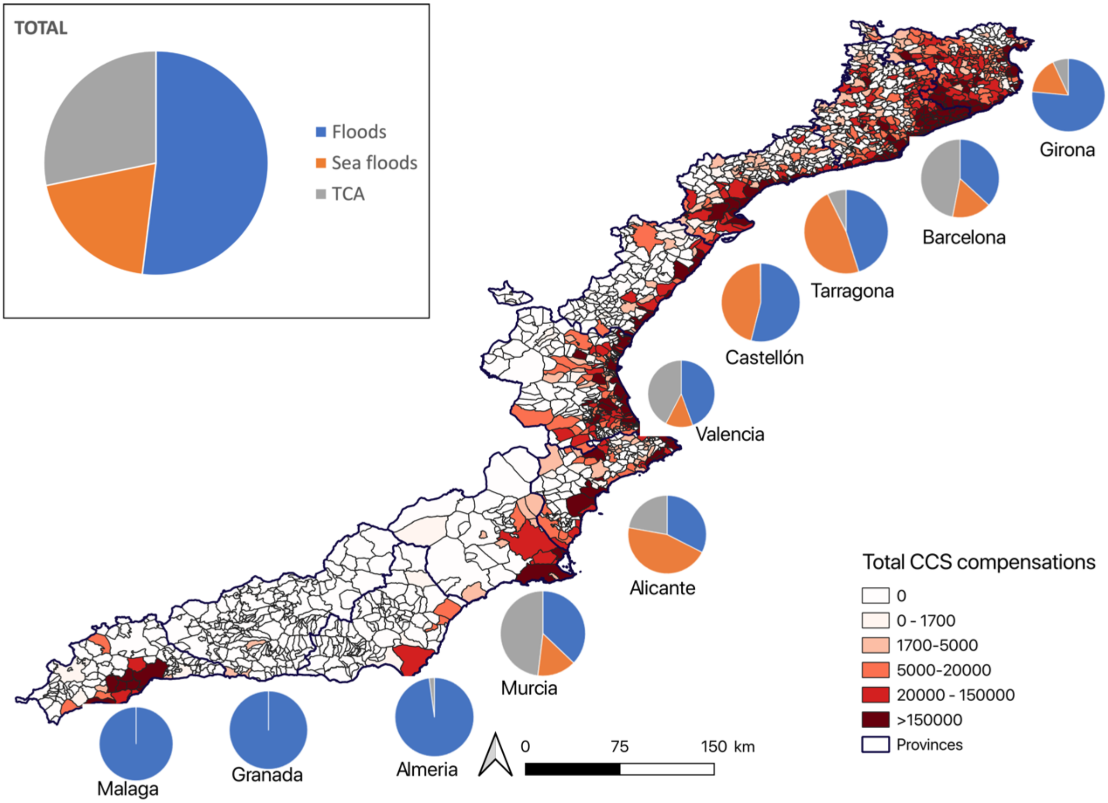

Figure 11: Map of the total compensation for floods, coastal flooding and windstorm (TCA) by municipality, with pie charts showing the distribution of compensation by cause at the province level.

Flood-related compensation dominated in most provinces, either alone or in combination with sea storms. This pattern was particularly marked in the Andalusian provinces, where compensation was almost entirely flood-related: 100% in Granada, 99.9% in Málaga, and 98% in Almería, with only 0.03% and 2%, respectively, attributable to TCA (windstorms). Given that rainfall totals were lower in the southern sector and that GDP levels were not among the highest, the comparatively large flood-related compensation suggests a stronger role of exposure, particularly the occupation of flood-prone areas, and the high value of the insured assets, given that the region is home to some luxury residences. In contrast, coastal flooding accounted for a much larger proportion of total compensation in Catalonia and the Valencian Community (Fig. 11), reflecting the stronger influence of marine storm impacts along these coastlines.

At the municipal scale, more than half of all affected municipalities received compensation exclusively for flooding, whereas 18% experienced both flooding and wind-related damage, and 5% received compensation associated with all three hazard types. The pattern differs markedly for coastal municipalities, where compound impacts became considerably more common. Only 20% of coastal municipalities received compensation exclusively for flooding, whereas 42% were simultaneously affected by flooding and coastal flooding, 7% by floods and windstorms and 29% received compensation associated with flooding, coastal flooding, and wind-related damage. These results illustrate the widespread occurrence of multiple hazard impacts within coastal environments during Storm Gloria.

The municipalities receiving the highest total compensation were Barcelona (EUR_{2022} 24 million), Málaga (EUR_{2022} 13 million) and Malgrat de Mar (EUR_{2022} 10 million). In the case of Malgrat de Mar, this result is unsurprising given its location near the mouth of the Tordera River. For Barcelona, the high compensation is consistent with the intensity of rainfall and wind, the large exposed population, and the high value of exposed assets. Málaga, however, reflects a different configuration: although average GDP is lower, the presence of numerous high-value second homes in flood prone areas increased insured losses substantially. Overall, these results illustrate the complexity involved in interpreting impact patterns, which depend not only on hazard intensity but also on the spatial distribution and value of exposed elements.

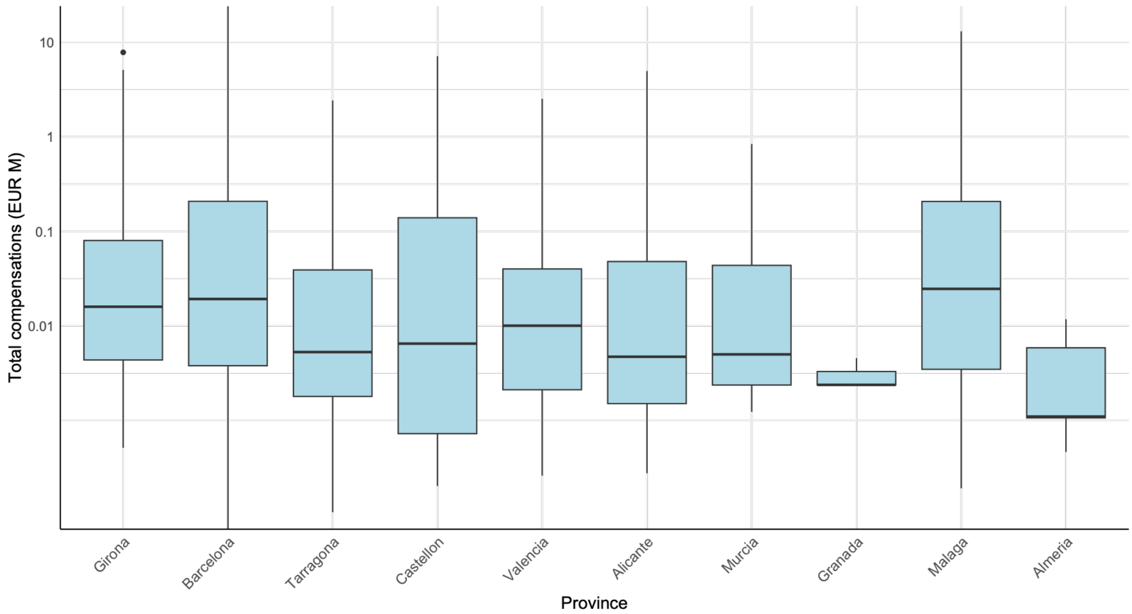

Figure 12: Distribution of total compensation paid to municipalities within each province. The y-axis is shown on a log10 scale with values expressed in EUR_{2022} million.

Figure 12 further shows substantial variability in compensation among municipalities within the same province. Málaga exhibits both the highest median compensation and the greatest dispersion of values, whereas Granada and Almería contain comparatively few municipalities with significant compensation payments This pattern reinforces the complexity of the hazard–impact relationship, which cannot be explained by hazard intensity alone but must also consider multiple factors related to exposure and vulnerability. Likewise, Figure 13 indicates that no single geographical pattern characterises the distribution of compensation among the three hazard categories.

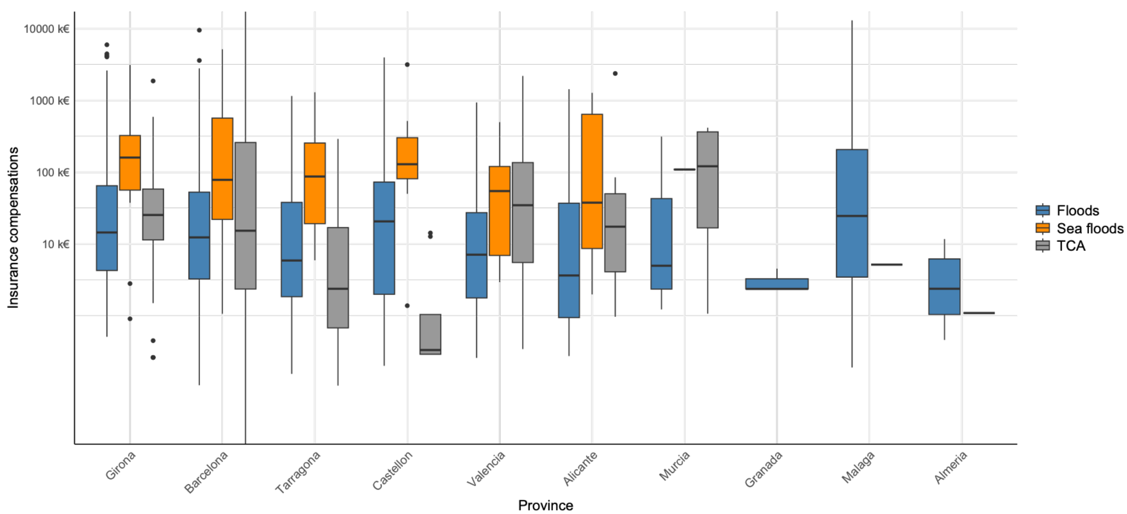

Figure 13: Distribution of compensation paid to each municipality located in each province, by hazard. In the case of Murcia, only two municipalities received compensation for coastal flooding, while in the Andalusian provinces, compensation was only related to floods, except in Almería and Málaga, where one municipality in each province received compensation for TCA (Atypical Cyclonic Storms).

To further examine the relationship between hazard intensity and economic losses, provinces were classified according to both meteorological severity and compensation level (Table 6). Hazard categories were derived from the maximum threshold exceeded by each meteorological variable, whereas compensation values were classified into terciles for each hazard type. Hazard categories are indicated as H1, H2 and H3, while compensation categories are indicated as C1, C2 and C3, corresponding respectively to low, intermediate and high levels. For each province and hazard type, the *hazard category* was then compared with the corresponding *compensation category*. Overall, a broadly consistent relationship emerges: provinces with the highest CCS payments generally correspond to category H3 in the hazard classification, indicating that at least two measurement points exceeded the highest threshold. One notable exception is Barcelona, where compensation related to coastal flooding reached the highest category, C3, even though the corresponding hazard was not classified at that level. This result, however, coincided with maximum-category values for the other two hazards and their associated CCS payments. Conversely, some provinces, such as Tarragona and Valencia, reached the highest hazard category without showing equally high compensation values. These discrepancies may reflect contextual factors that limited the resulting damage, including lower exposure or lower vulnerability in the affected areas.

Table 6: Hazard categories attained in each province according to the maximum threshold exceeded at a minimum of two stations or two SIMAR points for coastal flooding, and total compensation paid by hazard type and province, expressed in EUR_{2022} million (M). Ptotal: total precipitation, Wmax: maximum wind gust, Hs: sea wave height; CCS-Floods: compensation related to flooding; CCS-Sea floods: compensation related to sea floods; CCS-TCA: compensation related to wind-related claims.

Province	Ptotal	CCS-Floods (M)	Hs	CCS-Sea floods (M)	Wmax	CCS-TCA (M)
Girona	**H3**	**35.13 (C3)**	**H3**	**7.59 (C3)**	H1	3.20 (C2)
Barcelona	**H3**	**33.84 (C3)**	H2	**14.89 (C3)**	**H3**	**43.04 (C3)**
Tarragona	**H3**	5.01 (C2)	**H3**	5.29 (C2)	H1	0.81 (C1)
Castellón	**H3**	6.16 (C2)	H1	5.23 (C2)	H2	0.03 (C1)
Valencia	**H3**	**6.98 (C3)**	**H3**	2.07 (C2)	**H3**	6.66 (C2)
Alicante	**H3**	3.81 (C2)	**H3**	5.32 (C2)	H2	2.60 (C2)
Murcia	H2	0.63 (C1)	H1	0.25 (C1)	H2	0.81 (C1)
Almería	H1	0.05 (C1)	H1	-	H2	0.001 (C1)
Granada	H1	0.009 (C1)	H1	-	-	-
Málaga	**H3**	**14.93 (C3)**	H1	-	-	0.005 (C1)

7 Conclusions

Storm Gloria represents one of the most remarkable recent examples of compound flooding affecting the Spanish Mediterranean coast. Between 19 and 25 January precipitation was widespread, exceeding 500 mm at numerous stations (maximum of 527.5 mm). The event reached its peak between 19 and 21 January, when several stations recorded daily precipitation totals exceeding 250 mm, wind gusts above 110 km h^{-1} and maximum significant wave height above 8 m.

By combining meteorological observations, probabilistic analyses, documented impacts, and economic-loss data, this study provides an integrated assessment of how a single atmospheric episode generated multiple types of compound flood events and the consequences that followed. The results demonstrate that Storm Gloria simultaneously produced multivariate, spatially compound, and temporally compound flood events, each characterised by different physical mechanisms and distinct implications for emergency management. Multivariate events amplified impacts through the interaction of coincident fluvial and coastal processes at the same location, spatially compound events increased the geographical footprint of the emergency by simultaneously affecting different sectors of the coast, and temporally compound events intensified impacts because recovery from previous floods had not been completed. Together, these examples show that different compound-event types may coexist within a single storm and jointly contribute to the overall severity of the disaster.

The probabilistic analyses further demonstrate the importance of explicitly accounting for dependence between hazard drivers. For both the multivariate and spatially compound examples, considering statistical dependence substantially reduced the estimated joint return periods compared with the assumption of independence, confirming that conventional univariate approaches may considerably underestimate the likelihood of compound extremes.

The comparison between meteorological severity and economic compensation also highlights that hazard intensity alone is insufficient to explain disaster losses. Although the largest compensation payments generally occurred in areas experiencing the highest hazard levels, important regional differences emphasise the controlling influence of exposure and vulnerability. Moreover, while flooding accounted for most insured losses at the regional scale, coastal flooding became nearly as important as wind-related damage when only coastal municipalities were considered, underscoring the need to explicitly include marine processes in coastal flood-risk assessments.

Beyond direct economic losses, Storm Gloria generated numerous cascading impacts that persisted well beyond the meteorological event itself. Damage to transport infrastructure, beaches, ports, and coastal ecosystems required recovery periods extending over several years, while reconstruction efforts were further complicated by the onset of the COVID-19 pandemic shortly afterwards. At the same time, the event also generated beneficial geomorphological responses, including sediment redistribution within the Tordera delta and recharge of aquifers and reservoirs. These contrasting effects illustrate the dual role of extreme storms as both destructive events and natural agents of coastal morphodynamic adjustment, emphasising the need to evaluate both adverse and beneficial consequences when assessing coastal resilience.

From a management perspective, Storm Gloria exposed important limitations in current approaches to coastal flood risk. While emergency response was initially coordinated at municipal level, the large geographical footprint of the storm rapidly exceeded local response capacity and required increasing regional and national coordination. The event also placed considerable pressure on institutional mechanisms, including the Insurance Compensation Consortium, whose operational capacity had already been affected by previous flood events during late 2019. These observations highlight that compound events should be viewed not only as physical phenomena but also as governance challenges requiring coordination across administrative boundaries and throughout the entire disaster-management cycle, from preparedness to long-term recovery.

Beyond the specific case of Storm Gloria, this study demonstrates the value of integrating hazard characterisation, probabilistic dependence analysis, and observed impacts within a common framework for the analysis of compound events. Such an approach provides a more realistic representation of coastal flood risk than analysing individual hazards independently and offers a practical basis for improving early-warning systems, emergency planning, and long-term adaptation strategies. The framework presented here provides a practical basis for incorporating compound-event thinking into coastal flood-risk assessment and adaptation planning, an increasingly important requirement for climate-resilient management of Mediterranean and other vulnerable coastal regions.

Although this episode has been shown to be a paradigmatic case of different types of compound events, it was not a typical Mediterranean flood event. Such events usually occur in autumn and are mainly characterised by flash flooding. The magnitude and uniqueness of the event can be considered aligned with the consequences of climate change. This underscores the need to be prepared for unprecedented situations, as proposed by Kreibich et al. (2022).

Code and data availability

Meteorological data used in this study are available from the Spanish Meteorological Agency (AEMET, Agencia Estatal de Meteorología, link: https://www.aemet.es/en/datos_abiertos); SIMAR wave data, from Puertos del Estado (https://www.puertos.es/en/services/oceanography); CoExMed wave reanalysis from Toomey et al. (2022); financial compensation data from the Insurance Compensation Consortium (https://www.consorseguros.es/en/); flood episodes data from INUNGAMA (https://agora.ub.edu).

Author contributions

MLB: conceptualization, formal analysis, data curation, and visualization, writing-original draft, review/editing. RMM: writing-original draft, review/editing. MAV: coastal hazard characterization and probabilistic analysis. JAJ conceptualization, results evaluation and discussion, project management and funding, writing -review/editing. MCL: conceptualization, results evaluation and discussion, project management and funding, supervision, writing-original draft, review/editing.

Competing interests

The authors have the following competing interests: At least one of the (co-)authors is a member of the editorial board of Natural Hazards and Earth System Sciences

Disclaimer

Copernicus Publications remains neutral with regard to jurisdictional claims made in the text, published maps, institutional affiliations, or any other geographical representation in this paper. While Copernicus Publications makes every effort to include appropriate place names, the final responsibility lies with the authors. Views expressed in the text are those of the authors and do not necessarily reflect the views of the publisher.

Acknowledgements

We thank Tim Toomey and Marta Marcos (Universitat de les Illes Balears), Puertos del Estado and AEMET for providing access to wave and meteorological data used in this study, and CCS, and La Vanguardia for the information on impacts. RMM is a Serra Húnter fellow. MAV benefited from a Ph D grant from the Spanish Ministry of Science and Innovation. JAJ acknowledges the support of the Departament de Recerca i Universitats of the Generalitat de Catalunya (Acadèmia d'Excel·lència award, 2025ICREA00154). The work of MAV and JAJ was done within the C3RiskMed research project (grant no. PID2020-113638RB-C21, AEI/10.13039/501100011033)

Financial support

This work has been supported by the Spanish Project C3RiskMed (grants no. PID2020-113638RB-C22, AEI/10.13039/501100011033) and the INUND-IA project (RDI001/24/000013 financed by the Catalan Water Agency).

References

AEMET: Informe sobre borrascas y Gloria, https://www.aemet.es/ca/conocermas/borrascas/2019-2020 (last access: 25 March 2025), 2025.

AEMET: Informe de episodio de precipitaciones intensas en Málaga el día 25 de enero de 2020, 2020a.

AEMET: Informe de episodio meteorológico de temporal invernal (fecha de elaboración: 27/01/2020), 2020b.

Aguilera-Vidal, M., Sanuy, M., and Jiménez, J.A.: Beyond localized hotspots: hazard connectivity in spatially compound rainfall-coastal storm events. Environ. Res. Lett., 21, 144021, https://doi.org/10.1088/1748-9326/ae8a69, 2026.

Aguilera-Vidal, M., Sanuy, M., Ortego, M.I., and Jiménez, J.A.: Rainfall and wave storms interdependence in the western Spanish Mediterranean coast. J. Hydrol.: Reg. Stud., 62, 102873, https://doi.org/10.1016/j.ejrh.2025.102873, 2025.

Amaro, J., Gayà, M., Aran, M., and Llasat, M. C.: Preliminary results of the Social Impact Research Group of MEDEX: The request database (2000-2002) of two Meteorological Services, Nat. Hazards Earth Syst. Sci., 10, 2643–2652, https://doi.org/10.5194/nhess-10-2643-2010, 2010.

Amores, A., Marcos, M., Carrió, D. S., and Gómez-Pujol, L.: Coastal impacts of Storm Gloria (January 2020) over the north-western Mediterranean, Nat. Hazards Earth Syst. Sci., 20, 1955–1968, https://doi.org/10.5194/nhess-20-1955-2020, 2020.

Bevacqua, E., Maraun, D., Vousdoukas, M. I., Voukouvalas, E., Vrac, M., Mentaschi, L., and Widmann, M.: Higher probability of compound flooding from precipitation and storm surge in Europe under anthropogenic climate change, Sci. Adv., 5, eaaw5531, https://doi.org/10.1126/sciadv.aaw5531, 2019.

Camus, P., Haigh, I.D., Nas, A.A., Wahl, T., Darby, S.E. and Nicholls, R.J.: Regional analysis of multivariate compound coastal flooding potential around Europe and environs: sensitivity analysis and spatial patterns, Nat. Hazards Earth Syst. Sci., 21, 2021-2040; https://doi.org/10.5194/nhess-21-2021-2021, 2021.

Canals, M. and Miranda, J.: Sobre el temporal Gloria (19-23.01.20), els seus efectes sobre el país i el que se'n deriva, Report de Resposta Ràpida, edited by: Canals Artigas, M. and Miranda i Canals, J., 201 pp., 2020.

Coles, S.G. and Tawn, J.A.: Modelling extreme multivariate events, J. R. Statist. Soc., B 53, 377–392, https://doi.org/10.1111/j.2517-6161.1991.tb01830.x, 1991.

Coles, S., Heffernan, J. and Tawn, J.: Dependence Measures for Extreme Value Analyses, Extremes, 2, 339–365, https://doi.org/10.1023/A:1009963131610, 1999.

Comisionado del Gobierno frente al Reto Demográfico (CGRD): Diagnóstico: Estrategia Nacional frente al Reto Demográfico. Eje Efectos de la Población Flotante, Ministerio para la Transición Ecológica y el Reto Demográfico, https://www.miteco.gob.es/content/dam/miteco/es/reto-demografico/temas/analisis-cartografia/diagnostico_eje_flotante_tcm30-517771.pdf (last access: 25 September 2025), 2019.

Cortès, M., Turco, M., Llasat-Botija, M., and Carmen Llasat, M.: The relationship between precipitation and insurance data for floods in a Mediterranean region (northeast Spain), Nat. Hazards Earth Syst. Sci., 18, 857–868, https://doi.org/10.5194/nhess-18-857-2018, 2018.

Cortès, M., Turco, M., Ward, P., Sánchez-Espigares, J. A., Alfieri, L., and Llasat, M. C.: Changes in flood damage with global warming on the eastern coast of Spain, Nat. Hazards Earth Syst. Sci., 19, 2855–2877, https://doi.org/10.5194/nhess-19-2855-2019, 2019.

De Alfonso, M., Lin-Ye, J., García-Valdecasas, JM., Pérez-Rubio, S., Luna, MY., Santos-Muñoz, D., Ruiz, MI., Pérez-Gómez, B and Álvarez-Fanjul, E.: Storm Gloria: Sea State Evolution Based on in situ Measurements and Modeled Data and Its Impact on Extreme Values, Front. Mar. Sci., 8, 646873, https://doi.org/10.3389/fmars.2021.646873, 2021.

Del Río, L., Plomaritis, T. A., Benavente, J., Valladares, M., and Ribera, P.: Establishing storm thresholds for the Spanish Gulf of Cádiz coast, Geomorphology, 143–144, 13–23, https://doi.org/10.1016/j.geomorph.2011.04.048, 2012.

Del Rosal Salido, J., Bermudez, M., Ortega, M., Sanuy, M., Silva-Santana, M., and Jiménez, J.A.: A composite index framework for compound flood risk assessment, Comm. Earth Environ., 6, 342, doi: 10.1038/s43247-025-02331-z, 2025.

de Ruiter, M.C., Couasnon, A., van den Homberg, M.J.C., Daniell, J.E., Gill, J.C., and Ward, P.J.: Why we can no longer ignore consecutive disasters, Earth's Future, 8, e2019EF001425, https://doi.org/10.1029/2019EF001425, 2020.

Genest, C. and Favre, A.-C.: Everything you always wanted to know about copula modeling but were afraid to ask, J. Hydrol. Eng., 12, 347–368, https://doi.org/10.1061/(ASCE)1084-0699(2007)12:4(347), 2007.

Gobierno de España: Informe sobre el temporal de lluvia, nieve, viento y fenómenos costeros acaecido en el este peninsular y Baleares como consecuencia de la borrasca “Gloria”, La Moncloa, https://www.lamoncloa.gob.es/consejodeministros/Paginas/enlaces/280120-enlace-gloria.aspx, last access: 19 June 2026, 2020.

González, M. (coord.): El temporal Gloria (19-23/01/2020): els efectes dels processos geològics sobre el territori, Institut Cartogràfic i Geològic de Catalunya, Barcelona, 122 pp., 2020.

Green, J., Haigh, I. D., Quinn, N., Neal, J., Wahl, T., Wood, M., Eilander, D., de Ruiter, M., Ward, P., and Camus, P.: Review article: A comprehensive review of compound flooding literature with a focus on coastal and estuarine regions, Nat. Hazards Earth Syst. Sci., 25, 747-816, https://doi.org/10.5194/nhess-25-747-2025, 2025.

Haigh, I.D., Wadey, M.P., Wahl, T., Ozsoy, O., Nicholls, R.J., Brown, J.M., Horsburgh, K. and Gouldby, B.: Spatial and temporal analysis of extreme sea level and storm surge events around the coastline of the UK, Sci. Data, 3, 160107, https://doi.org/10.1038/sdata.2016.107, 2016.

Iglesias, J., Cuesta, I., Salueña, C., Moré, J., and Solé, J.: Analysis and comparison of coupled and uncoupled simulations with the COAWST model during the Gloria Storm (January 2020) in the northwestern Mediterranean Sea, Environ. Model. Softw., 169, 105830, https://doi.org/10.1016/j.envsoft.2023.105830, 2023.

IPCC: Managing the Risks of Extreme Events and Disasters to Advance Climate Change Adaptation. A Special Report of Working Groups I and II of the Intergovernmental Panel on Climate Change (IPCC), Cambridge University Press, Cambridge, UK, and New York, NY, USA, 582 pp., 2012.

Jiménez, J. A., Sanuy, M., Ballesteros, C., and Valdemoro, H. I.: The Tordera Delta, a hotspot to storm impacts in the coast northwards of Barcelona (NW Mediterranean), Coast. Eng., 134, 148–158, https://doi.org/10.1016/j.coastaleng.2017.08.012, 2018.

Khodayar, S., Kushta, J., Catto, J. L., Dafis, S., Davolio, S., Ferrarin, C., Flaounas, E., Groenemeijer, P., Hatzaki, M., Hochman, A., Kotroni, V., Landa, J., Láng-Ritter, I., Lazoglou, G., Liberato, M. L. R., Miglietta, M. M., Papagiannaki, K., Patlakas, P., Stojanov, R., and Zittis, G.: Mediterranean cyclones in a changing climate: a review on their socio-economic impacts, Rev. Geophys., 63, e2024RG000853, https://doi.org/10.1029/2024RG000853, 2025.

Kreibich, H., Van Loon, A. F., Schröter, K., Ward, P. J., Mazzoleni, M., Sairam, N., Abeshu, G. W., Agafonova, S., AghaKouchak, A., Aksoy, H., Alvarez-Garreton, C., Aznar, B., Balkhi, L., Barendrecht, M. H., Biancamaria, S., Bos-Burgering, L., Bradley, C., Budiyono, Y., Buytaert, W., Capewell, L., Carlson, H., Cavus, Y., Couasnon, A., Coxon, G., Daliakopoulos, I., de Ruiter, M. C., Delus, C., Erfurt, M., Esposito, G., François, D., Frappart, F., Freer, J., Frolova, N., Gain, A. K., Grillakis, M., Grima, J. O., Guzmán, D. A., Huning, L. S., Ionita, M., Kharlamov, M., Khoi, D. N., Kieboom, N., Kireeva, M., Koutroulis, A., Lavado-Casimiro, W., Li, H.-Y., Llasat, M. C., Macdonald, D., Mård, J., Mathew-Richards, H., McKenzie, A., Mejia, A., Mendiondo, E. M., Mens, M., Mobini, S., Mohor, G. S., Nagavciuc, V., Ngo-Duc, T., Nguyen Huynh, T. T., Nhi, P. T. T., Petrucci, O., Nguyen, H. Q., Quintana-Seguí, P., Razavi, S., Ridolfi, E., Riegel, J., Sadik, M. S., Savelli, E., Sazonov, A., Sharma, S., Sörensen, J., Souza, F. A. A., Stahl, K., Steinhausen, M., Stoelzle, M., Szalińska, W., Tang, Q., Tian, F., Tokarczyk, T., Tovar, C., Tran, T. V. T., Van Huijgevoort, M. H. J., van Vliet, M. T. H., Vorogushyn, S., Wagener, T., Wang, Y., Wendt, D. E., Wickham, E., Yang, L., Zambrano-Bigiarini, M., Blöschl, G., and Di Baldassarre, G.: The challenge of unprecedented floods and droughts in risk management, Nature, 608, 80–86, https://doi.org/10.1038/s41586-022-04917-5, 2022.

Leeding, R., Riboldi, J., and Messori, G.: On Pan-Atlantic cold, wet and windy compound extremes, Weather Clim. Extrem., 39, https://doi.org/10.1016/j.wace.2022.100524, 2022.

Leonard, M., Westra, S., Phatak, A., Lambert, M. F., van den Hurk, B., McInnes, K. L., Risbey, J. S., Schuster, S., Jakob, D., and Stafford-Smith, M.: A compound event framework for understanding extreme impacts, WIREs Clim. Change, 5, 113–128, https://doi.org/10.1002/wcc.252, 2014.

Llasat, M.C., Llasat-Botija, M., Pardo, E., and Esbrí, L.: Informe tècnic de l’episodi d’inundacions del 19 a 23 de gener de 2020, Informe d’Estudi Projecte Agora 22, Universitat de Barcelona, https://agora.ub.edu/portal-historic/, last access: 13 February 2026, 2023.

Luján López, A.: Las siniestralidades de Gloria, Consorseguros: Revista Digital, 16, 1–14, https://www.consorsegurosdigital.com/es/numero-16/sumario/colaboraciones/las-siniestralidades-de-gloria/, last access: 13 February 2026, 2022.

Marco-Méndez, C., Marbà, N., Amores, Á., Romero, J., Minguito-Frutos, M., García, M., Pagès, J. F., Prado, P., Boada, J., Sánchez-Lizaso, J. L., Ruiz, J. M., Muñoz-Ramos, G., Sanmartí, N., Mayol, E., Buñuel, X., Bernardeau-Esteller, J., Navarro-Martinez, P. C., Marín-Guirao, L., Morell, C., Wesselmann, M., Font, R., Hendriks, I. E., Seglar, X., Camps-Castella, J., Bonfill, E., Requena-Gutiérrez, A., Blanco-Murillo, F., Aguilar-Escribano, J., Jimenez-Gutierrez, S., Martínez-Vidal, J., Guillén, J. E., Cefalì, M. E., Pérez, M., Marcos, M., and Alcoverro, T.: Evaluating the extent and impact of the extreme Storm Gloria on Posidonia oceanica seagrass meadows, Sci. Total Environ., 908, 168404, https://doi.org/10.1016/j.scitotenv.2023.168404, 2024.

MedECC: Summary for Policymakers, in: Climate and Environmental Coastal Risks in the Mediterranean, edited by: Djoundourian, S., Lionello, P., Llasat, M. C., Guiot, J., Cramer, W., Driouech, F., Gattacceca, J. C., and Marini, K., MedECC Reports, MedECC Secretariat, Marseille, France, 28 pp., ISBN 978-2-493662-03-3, https://doi.org/10.5281/zenodo.10722133, 2024.

Mendoza, E. T., Jimenez, J. A. and Mateo, J.: A coastal storms intensity scale for the Catalan Sea (NW Mediterranean), Nat. Hazards Earth Syst. Sci. 11.9, 2453-2462, https://doi.org/10.5194/nhess-11-2453-2011, 2011.

Messner, F. and Meyer, V.: Flood damage, vulnerability and risk perception – challenges for flood damage research, in: Flood Risk Management: Hazards, Vulnerability and Mitigation Measures, edited by: Schanze, J., Zeman, E., and Marsalek, J., NATO Science Series IV: Earth and Environmental Sciences, 67, Springer, Dordrecht, the Netherlands, 149–167, https://doi.org/10.1007/978-1-4020-4598-1_13, 2006.

Moftakhari, H.R., Salvadori, G., AghaKouchak, A., Sanders, B.F., and Matthew, R.A.: Compounding effects of sea level rise and fluvial flooding, P. Natl. Acad. Sci., USA, 114, 9785–9790, https://doi.org/10.1073/pnas.1620325114, 2017.

Nagler, T., Schepsmeier, U., Stoeber, J., Brechmann, E. C., Graeler, B., and Erhardt, T.: VineCopula: Statistical Inference of Vine Copulas, R package version 2.6.1, https://doi.org/10.32614/CRAN.package.VineCopula, 2025.

National Academies of Sciences, Engineering, and Medicine (NASEM): Resilience for Compounding and Cascading Events, The National Academies Press, Washington, DC, USA, 68 pp., https://doi.org/10.17226/26659, 2022.

OCCC (Oficina Catalana del Canvi Climàtic): L'impacte de la tempesta Glòria, Generalitat de Catalunya, 6 pp., https://canviclimatic.gencat.cat/web/.content/03_AMBITS/adaptacio/ESCACC_2021_2030/Informe-Gloria.pdf, last access: 13 February 2026, 2020.

Palau, R.M., Berenguer, M., Hürlimann, M., and Sempere-Torres, D.: Application of a fuzzy verification framework for the evaluation of a regional-scale landslide early warning system during the January 2020 Gloria storm in Catalonia (NE Spain), Landslides, 19, 1599–1616, 2022.

Pantaleoni Reluy, N., Hürlimann, M., and Lantada, N.: How are public compensation efforts implemented in multi-hazard events? Insights from the 2020 Gloria storm in Catalonia, Nat. Hazards Earth Syst. Sci., 25, 3483–3504, https://doi.org/10.5194/nhess-25-3483-2025, 2025.

Pérez-Gómez, B., García-León, M., García-Valdecasas, J., Clementi, E., Mösso Aranda, C., Pérez-Rubio, S., Masina, S., Coppini, G., Molina-Sánchez, R., Muñoz-Cubillo, A., García Fletcher, A., Sánchez González, J.F., Sánchez-Arcilla, A., and Álvarez Fanjul, E.: Understanding Sea Level Processes During Western Mediterranean Storm Gloria, Front. Mar. Sci., 8, 647437, https://doi.org/10.3389/fmars.2021.647437, 2021.

Petrucci, O. and Llasat, M. C.: Impact of disasters in Mediterranean regions: an overview in the framework of the HYMEX project, in: Landslide Science and Practice, Vol. 7: Social and Economic Impact and Policies, edited by: Margottini, C., Canuti, P., and Sassa, K., Springer, Berlin and Heidelberg, Germany, 137–143, https://doi.org/10.1007/978-3-642-31313-4_18, 2013.

Pintó, J., Garcia-Lozano, C., Sardá, R., Roig-Munar, F. X., and Martí, C.: Efectes del temporal Glòria sobre el litoral, Treb. Soc. Catalana Geogr., 89, 89–109, https://doi.org/10.2436/20.3002.01.192, 2020.

Rivas, V., Garmendia, C., and Rasilla, D.: Analysis of ocean parameters as sources of coastal storm damage: regional empirical thresholds in northern Spain, Climate, 10, 88, https://doi.org/10.3390/cli10060088, 2022.

ROM: Recomendaciones de Obras Marítimas 0.3 Wave Annex E1. Wave climate of the Spanish coast. Puertos del Estado, 1991.

Romero-Martín, R., Caballero-Leiva, I., Llasat, M.C., Llasat-Botija, M., Rigo, T., Valdemoro, H.I., Gilabert, J., Cortès, M., and Jiménez, J.A.: Mapping cumulative compound hydrometeorological and marine-induced risks on the NW Mediterranean coast, Sci. Rep., 14, 3237, https://doi.org/10.1038/s41598-024-53899-z, 2024.

Romero-Martín, R., Sanuy, M., and Jiménez, J.A.: Unveiling the role of storm surges as a driver of flooding on the western Mediterranean: a case study of the Ebro Delta, Nat. Hazards, 121, 4961–4984, https://doi.org/10.1007/s11069-024-06984-5, 2025.

Santasusagna Riu, A. and Tort Donada, J.: El temporal Glòria: consideracions sobre la seva afecció a la Costa Central Catalana, Treballs de la Societat Catalana de Geografia, 89, 191–220, https://doi.org/10.2436/20.3002.01.196, 2020.

Sanuy, M., and Jiménez, J.A.: Probabilistic characterisation of coastal storm-induced risks using Bayesian networks, Nat. Hazards Earth Syst. Sci., 21, 219–238, https://doi.org/10.5194/nhess-21-219-2021, 2021.

Sanuy, M., Rigo, T., Jiménez, J. A., and Llasat, M. C.: Classifying compound coastal storm and heavy rainfall events in the north-western Spanish Mediterranean, Hydrol. Earth Syst. Sci., 25, 3759–3781, https://doi.org/10.5194/hess-25-3759-2021, 2021.

Seneviratne, S.I. et al.: Changes in climate extremes and their impacts on the natural physical environment. In: Field, C.B. et al. (Eds), Managing the Risks of Extreme Events and Disasters to Advance Climate Change Adaptation. A Special Report of Working Groups I and II of the Intergovernmental Panel on Climate Change (IPCC), Cambridge University Press, Cambridge, UK, and New York, NY, USA, 109–230, https://doi.org/10.7916/d8-6nbt-s431, 2012.

Shan, B., Verhoest, N.E.C., and De Baets, B.: Identification of compound drought and heatwave events on a daily scale and across four seasons, Hydrol. Earth Syst. Sci., 28, 2065–2080, https://doi.org/10.5194/hess-28-2065-2024, 2024.

SMC (Servei Meteorològic de Catalunya): Balanç d'una llevantada històrica a Catalunya, 1–11 pp., 2020.

Sotillo, M.G., Mourre, B., Mestres, M., Lorente, P., Aznar, R., García-León, M., Liste, M., Santana, A., Espino, M., and Álvarez, E.: Evaluation of the Operational CMEMS and Coastal Downstream Ocean Forecasting Services During the Storm Gloria (January 2020), Front. Mar. Sci., 8: 644525, https://doi.org/10.3389/fmars.2021.644525, 2021.

Toomey, T., Amores, A., Marcos, M., and Orfila, A.: Coastal sea levels and wind-waves in the Mediterranean Sea since 1950 from a high-resolution ocean reanalysis, Front. Mar. Sci., 9, https://doi.org/10.3389/fmars.2022.991504, 2022.

MITECO (Ministerio para la Transición Ecológica y el Reto Demográfico): Guías de adaptación al riesgo de inundación: edificaciones, caso piloto: Ayuntamiento de Los Alcázares (Murcia), Dirección General del Agua, 29 pp., https://www.miteco.gob.es/content/dam/miteco/es/agua/temas/gestion-de-los-riesgos-de-inundacion/4-ayuntamiento-losalcazares-murcia_tcm30-530660.pdf, last access: 13 February 2026, 2020.

Wahl, T., Jain, S., Bender, J., Meyers, S. D., and Luther, M. E.: Increasing risk of compound flooding from storm surge and rainfall for major US cities, Nature Climate Change, 5, 1093–1097, https://doi.org/10.1038/nclimate2736, 2015.

Zscheischler, J., Martius, O., Westra, S., Bevacqua, E., Raymond, C., Horton, R. M., van den Hurk, B., AghaKouchak, A., Jézéquel, A., Mahecha, M. D., Maraun, D., Ramos, A. M., Ridder, N. N., Thiery, W., and Vignotto, E.: A typology of compound weather and climate events, Nat Rev Earth Environ, 1, 333–347, https://doi.org/10.1038/s43017-020-0060-z, 2020.

Appendix A. Complementary tables and maps

Table A1. Stations that recorded maximum wind gusts above 90 km h^{-1} between 19 and 21 January *(Coordinates in decimal degrees, WGS84 (EPSG:4326))

Coordinates (Lat, Lon)*	Station name (altitude in m)	Province	19/1	20/1	21/1
38.28º N, 0.57º W	Alicante-Elche aeropuerto (43)	Alicante		94	
41.41º N, 2.12º E	Barcelona - Fabra (408)	Barcelona	91	103	104
41.39º N, 2.2º E	Barcelona - CMT (6)	Barcelona	91	106	
41.29º N, 2.07º E	Barcelona - Aeropuerto (4)	Barcelona		105	
39.01ºN, 0.30º W	Barx (340)	Valencia	108	96	
36.72º N, 2.19º W	Cabo de Gata - Faro (52)	Almería		103	
38.78º N, 0.16º E	Jávea -Ayuntamiento (15)	Alicante	93	94	
37.03º N, 2.91º W	Lújar de Andarax (1518)	Almería	93		
40.69º N, 0.16º E	La Pobla de Benifassà (1168)	Castellón			104
42.38º N, 2.75º E	Maçanet de Cabrenys (355)	Girona	94		
41.17º N, 0.35º E	Massaluca (370)	Tarragona		91	
38.95º N, 0.13º W	Miramar - semiautomática (12)	Valencia	100	93	
40.62º N, 0.10º W	Morella - Paseo Alameda (990)	Castellón			97
37.77º N, 0.80º W	Murcia - San Javier II (4)	Murcia		104	
38.92º N, 0.09º W	Oliva (5)	Valencia		115	
41.41º N, 1.51º E	Pontons (632)	Barcelona		91	
37.69º N, 0.73º W	San Javier - La Manga (4)	Murcia	90	91	
39.48º N, 0.47º W	Valencia - Aeropuerto (56)	Valencia		96	
41.50º N, 2.36º E	Vilassar de Dalt (56)	Barcelona	102		

Table A2. Number of municipalities affected by flooding, coastal flooding, or TCA (windstorms), by coastal provinces and for the study area as a whole. *In the total figure for each region, each municipality is counted only once, even if it has been affected by one, two or three hazards.

	GI	BCN	TGN	CAST	VAL	ALIC	MURC	ALM	GRA	MAL	Total
Floods	172	182	68	31	127	66	15	7	3	21	692
Coastal floods	18	20	17	13	17	15	2	0	0	0	102
TCA	25	141	28	8	38	10	4	1	0	1	256
Total*	174	218	82	39	142	68	15	8	3	21	770

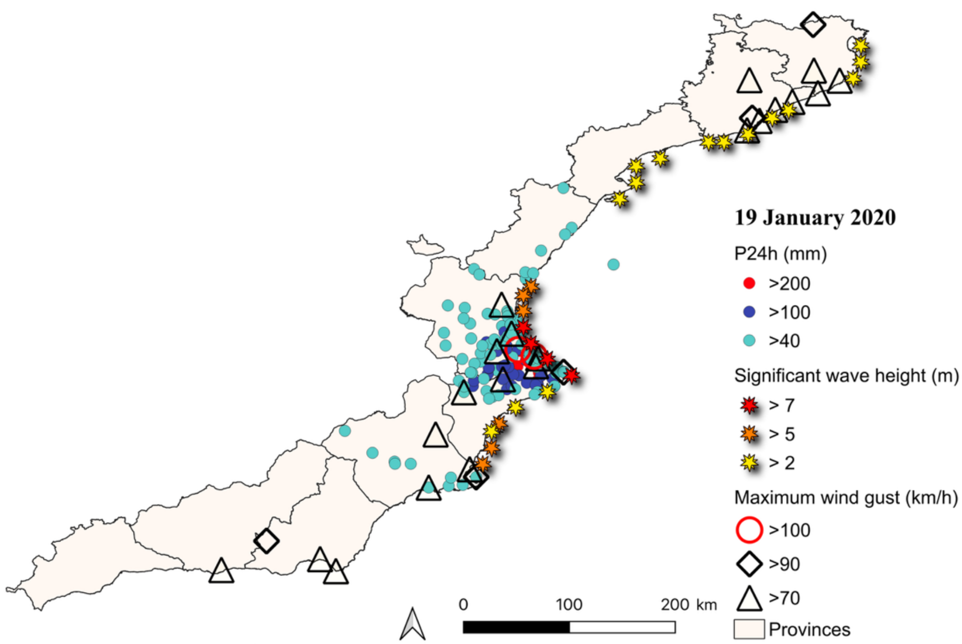

Figure A1. Stations where the wave height, maximum wind gusts and precipitation thresholds were exceeded on 19 January 2020.

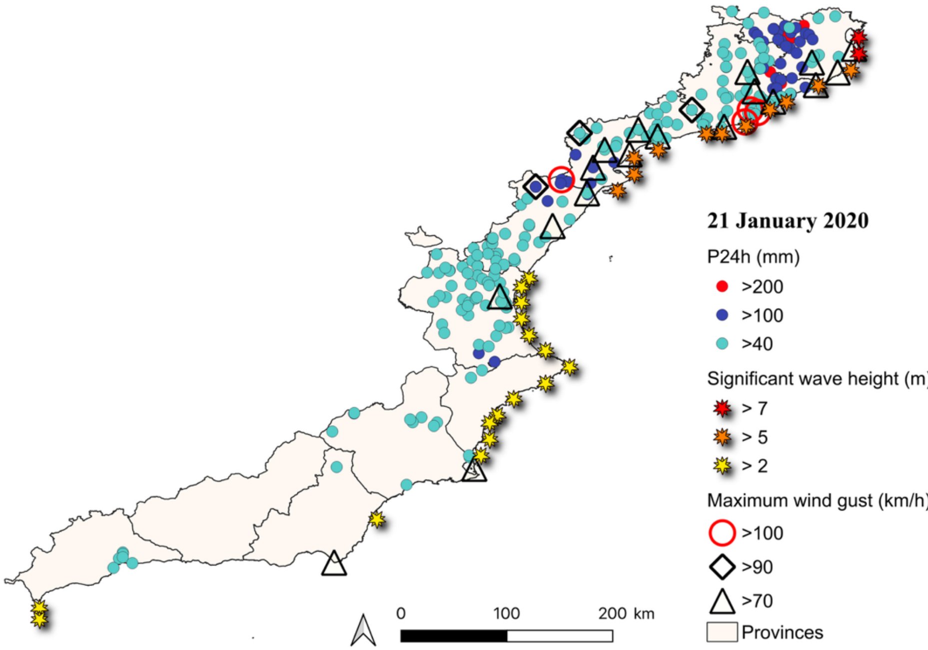

Figure A2. Stations where the wave height, maximum wind gusts and precipitation thresholds were exceeded on 21 January 2020.

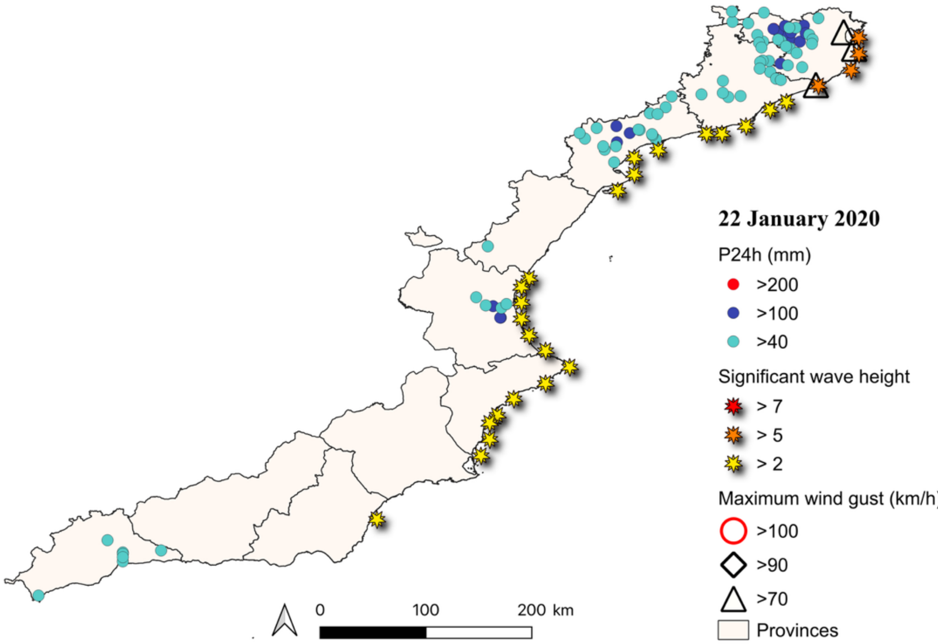

970 **Figure A3. Stations where the wave height, maximum wind gusts and precipitation thresholds were exceeded on 22 January 2020.**

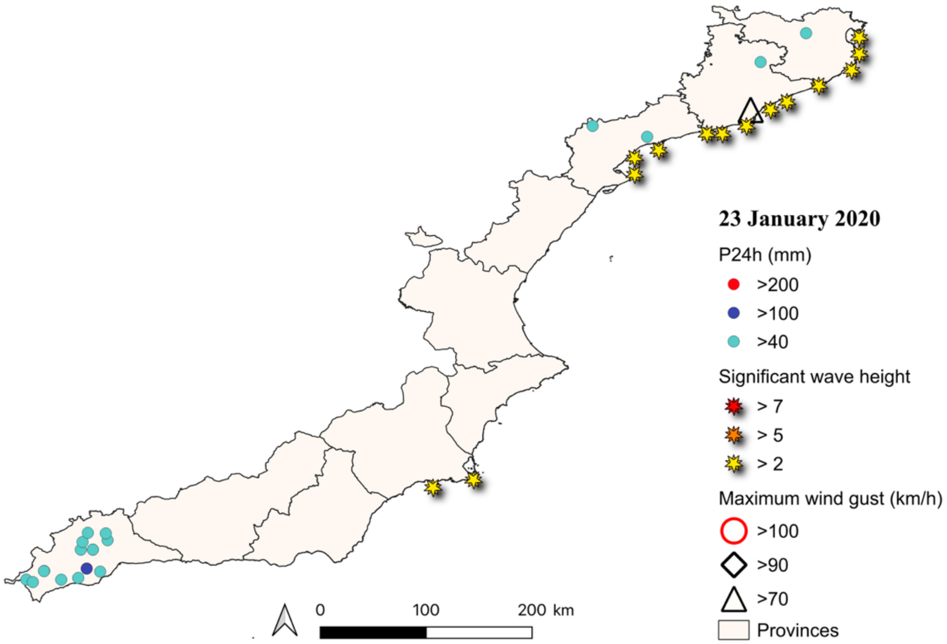

Figure A4. Stations where the wave height, maximum wind gusts and precipitation thresholds were exceeded on 23 January 2020.

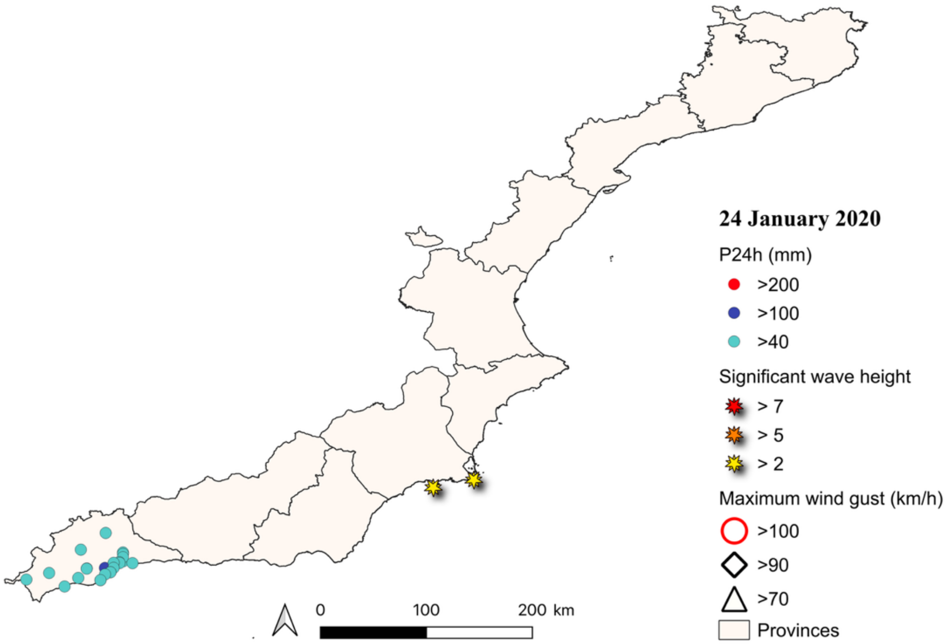

Figure A5. Stations where the wave height, maximum wind gusts and precipitation thresholds were exceeded on 24 January 2020.

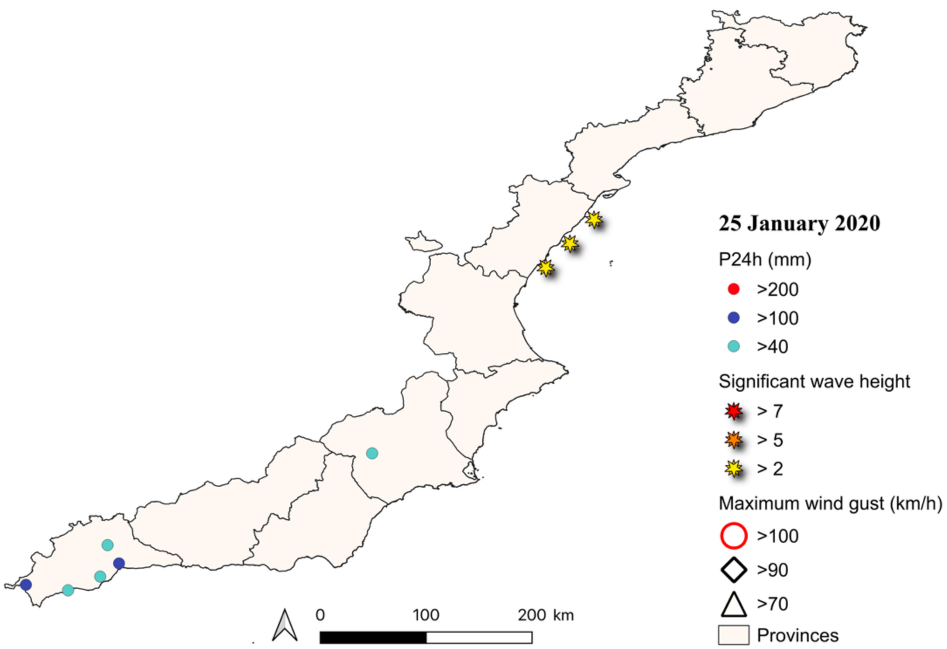

975

Figure A6. Stations where the wave height, maximum wind gusts and precipitation thresholds were exceeded on 25 January 2020.